A formula for the Θ-invariant from Heegaard diagrams

CHRISTINE LESCOP

The Θ-invariant is the simplest 3-manifold invariant defined with configuration space integrals. It is actually an invariant of rational homology spheres equipped with a combing over the complement of a point. It can be computed as the algebraic intersection of three propagators associated to a given combing X in the 2-point configuration space of a $\mathbb{Q}$–sphere M. These propagators represent the linking form of M so that $\Theta(M,X)$ can be thought of as the cube of the linking form of M with respect to the combing X. The invariant Θ is the sum of $6\lambda(M)$ and $\frac{p_1(X)}{4}$, where λ denotes the Casson-Walker invariant, and p_1 is an invariant of combings, which is an extension of a first relative Pontrjagin class. In this article, we present explicit propagators associated with Heegaard diagrams of a manifold, and we use these "Morse propagators", constructed with Greg Kuperberg, to prove a combinatorial formula for the Θ-invariant in terms of Heegaard diagrams.

57M27; 57N10, 55R80, 57R20

Contents

Published: XX Xxxember 20XX DOI: 10.2140/gt.20XX.XX.1001

1 Introduction

In this article, a $\mathbb{Q}$–*sphere* or *rational homology sphere* is a smooth closed oriented 3-manifold that has the same rational homology as S^3.

1.1 General introduction

The work of Witten [18] pioneered the introduction of many $\mathbb{Q}$–sphere invariants. The Le-Murakami-Ohtsuki universal finite type invariant [9] and the Kontsevich configuration space invariant [7], which was proved to be equivalent to the LMO invariant for integer homology spheres by G. Kuperberg and D. Thurston [8], are among them. The construction of the Kontsevich configuration space invariant for a $\mathbb{Q}$–sphere M involves a point ∞ in M, an identification of a neighborhood of ∞ with a neighborhood of ∞ in $S^3 = \mathbb{R}^3 \cup \{\infty\}$, and a parallelization τ of $(\check{M} = M \setminus \{\infty\})$ that coincides with the standard parallelization of $\mathbb{R}^3$ near ∞. The Kontsevich configuration space invariant is in fact an invariant of (M,τ). Its degree one part $\Theta(M,\tau)$ is the sum of $6\lambda(M)$ and $\frac{p_1(\tau)}{4}$, where λ is the Casson-Walker invariant and p_1 is a Pontrjagin number associated with τ, according to a Kuperberg Thurston theorem [8] generalized to rational homology spheres in [11]. Here, the Casson-Walker invariant λ is normalized as in [1, 3, 15] for integer homology spheres, and like $\frac{1}{2}\lambda_W$ for rational homology spheres where λ_W is the Walker normalisation in [16].

The invariant $\Theta(M,\tau)$ reads

$$\Theta(M,\tau) = \int_{\check{M}^2 \setminus \mathrm{diag}(\check{M})^2} \omega(M,\tau)^3$$

for some closed 2-form $\omega(M,\tau)$, which is often called a *propagator*. As it is developed in [11, Section 6.5], $\Theta(M,\tau)$ can also be written as the algebraic intersection of three 4-dimensional chains in a compactification $C_2(M)$ of $\check{M}^2 \setminus \mathrm{diag}(\check{M})^2$, for chains that are Poincaré dual to $\omega(M,\tau)$ in the 6–dimensional configuration space $C_2(M)$. In this article, a *propagator* will be such a 4-chain. For more precise definitions, see Subsection 2.2. A *combing* of a 3-manifold M as above is an asymptotically constant nowhere zero section of the tangent bundle to $\check{M}$.

In Theorem 2.1, we will prove that the invariant Θ is an invariant of combed $\mathbb{Q}$–spheres (M,X) rather than an invariant of parallelised punctured $\mathbb{Q}$–spheres, so that $(4\Theta(M,X) - 24\lambda(M))$ is an extension of the Pontrjagin number p_1 to combings. The invariant p_1 of parallelizations coincides with the Hirzebruch defect of the parallelization τ studied in [5, 6]. This invariant p_1 of combings is studied in [13], and it is shown to be the analogue of the Gompf θ-invariant [2, Section 4] of $\mathbb{Q}$–sphere combings, for asymptotically constant combings of punctured $\mathbb{Q}$–spheres. The variations of Θ, θ and p_1 under various combing changes are described in [13].

In Section 4, we describe explicit propagators associated with Morse functions or with Heegaard splittings. These "Morse propagators" have been obtained in collaboration with Greg Kuperberg. Then we use these propagators to produce a combinatorial description of Θ in terms of Heegaard diagrams in Theorem 3.8.

Our Morse propagators and our techniques could be applied to compute more configuration space invariants, and they might be useful to relate finite type invariants to Heegaard Floer homology.

This article benefited from the stimulating visit of Greg Kuperberg in Grenoble in 2010-2011. It also benefited from the referees' comments.

1.2 Conventions and notations

Unless otherwise mentioned, all manifolds are oriented. Boundaries are oriented by the outward normal first convention. Products are oriented by the order of the factors. More generally, unless otherwise mentioned, the order of appearance of coordinates or parameters orients manifolds or chains, which are linear combinations of manifolds. The fiber of the normal bundle $\mathfrak{V}(V)$ to an oriented submanifold V is oriented so that the normal bundle followed by the tangent bundle to the submanifold induce the orientation of the ambient manifold, fiberwise. The transverse intersection of two submanifolds V and W is oriented so that the normal bundle to $V \cap W$ is $(\mathfrak{V}(V) \oplus \mathfrak{V}(W))$, fiberwise. When the dimensions of two such submanifolds add up to the dimension of the ambient manifold U, each intersection point x is equipped with a sign ± 1 that is 1 if and only if $(\mathfrak{V}_x(V) \oplus \mathfrak{V}_x(W))$ (or equivalently $(T_x(V) \oplus T_x(W))$) induces the orientation of U. When V is compact, the sum of the signs of the intersection points is the *algebraic intersection number* $\langle V, W \rangle_U$. For a manifold V, $(-V)$ denotes the manifold V equipped with the opposite orientation.

2 The Θ-invariant

This section presents a complete definition of the invariant Θ.

2.1 On configuration spaces

In this article, *blowing up* a submanifold V means replacing it by its unit normal bundle. Locally, $\mathbb{R}^c \times V$ is replaced with $[0,\infty[\times S^{c-1}\times V$, where the fiber $\mathbb{R}^c$ of the normal bundle is naturally identified with $\{0\}\cup\left(]0,\infty[\times S^{c-1}\right)$. Topologically, this amounts to removing an open tubular neighborhood of the submanifold (thought of as infinitely small), but the process is canonical, so that the created boundary is the unit normal bundle to the submanifold and there is a canonical projection from the manifold obtained by blow-up to the initial manifold.

In a closed 3-manifold M, we fix a point ∞ and define the blown-up manifold $C_1(M)$ as the compact 3-manifold obtained from M by blowing up $\{\infty\}$. This space $C_1(M)$ is a compactification of $\check{M}=(M\setminus\{\infty\})$.

The *configuration space* $C_2(M)$ is the compact 6–manifold with boundary and corners obtained from M^2 by blowing up (∞,∞), and the closures of $\{\infty\}\times\check{M}$, $\check{M}\times\{\infty\}$ and the diagonal of $\check{M}^2$, successively.

Then the boundary $\partial C_2(M)$ of $C_2(M)$ contains the unit normal bundle to the diagonal of $\check{M}^2$. This bundle is canonically isomorphic to the unit tangent bundle $U\check{M}$ of $\check{M}$ via the map

$$[(x,y)]\in\frac{\frac{T_m\check{M}^2}{\text{diag}}\setminus\{0\}}{\mathbb{R}^{+*}}\mapsto[y-x]\in\frac{T_m\check{M}\setminus\{0\}}{\mathbb{R}^{+*}}.$$

When M is a rational homology sphere, the configuration space $C_2(M)$ has the same rational homology as S^2 (see the proof of Theorem 2.1 below) and $H_2(C_2(M);\mathbb{Q})$ has a canonical generator $[S]$ that is the homology class of a product $(x\times\partial B(x))$ where $B(x)$ is a ball embedded in $\check{M}$ that contains x in its interior. For a 2-component link (J,K) of M, the homology class $[J\times K]$ of $J\times K$ in $H_2(C_2(M);\mathbb{Q})$ reads $lk(J,K)[S]$, where $lk(J,K)$ is the *linking number* of J and K, which is the algebraic intersection number of J and a 2-dimensional chain bounded by K (see [12, Proposition 1.6]).

2.2 On propagators

When M is a rational homology sphere, a *propagator* of $C_2(M)$ is a 4–cycle $\mathcal{P}$ of $(C_2(M),\partial C_2(M))$ that is Poincaré dual to the preferred generator of $H^2(C_2(M);\mathbb{Q})$ that

maps $[S]$ to 1. For such a propagator $\mathcal{P}$, for any 2-cycle G of $C_2(M)$,

$$[G] = \langle \mathcal{P}, G\rangle_{C_2(M)}[S]$$

in $H_2(C_2(M);\mathbb{Q})$ where $\langle \mathcal{P}, G\rangle_{C_2(M)}$ denotes the algebraic intersection of $\mathcal{P}$ and G in $C_2(M)$.

Let B and $\frac{1}{2}B$ be two balls in $\mathbb{R}^3$ of respective radii R and $\frac{R}{2}$, centered at the origin in $\mathbb{R}^3$. Identify a neighborhood of ∞ in M with $S^3 \setminus (\frac{1}{2}B)$ in $(S^3 = \mathbb{R}^3 \cup \{\infty\})$ so that $\check{M}$ reads $\check{M} = B_M \cup_{]R/2,R]\times S^2} (\mathbb{R}^3 \setminus (\frac{1}{2}B))$ for a rational homology ball B_M whose complement in $\check{M}$ is identified with $\mathbb{R}^3 \setminus B$. There is a canonical regular map

$$p_\infty : (\partial C_2(M) \setminus UB_M) \to S^2$$

that maps the limit in $\partial C_2(M)$ of a convergent sequence of ordered pairs of distinct points of $\left(\check{M} \setminus B_M\right)^2$ to the limit of the direction from the first point to the second one. See [10, Lemma 1.1]. Let

$$\tau_s : \mathbb{R}^3 \times \mathbb{R}^3 \to T\mathbb{R}^3$$

denote the standard parallelization of $\mathbb{R}^3$. In this article, a *combing* X of a $\mathbb{Q}$–sphere M is a section of $U\check{M}$ that is constant outside B_M, i.e. that reads $\tau_s((\check{M} \setminus B_M) \times \{\vec{v}(X)\})$ for some fixed $\vec{v}(X) \in S^2$ outside B_M. The *propagator boundary* $\partial\mathcal{P}_X$ associated with such a combing X is the following 3–cycle of $\partial C_2(M)$

$$\partial\mathcal{P}_X = p_\infty^{-1}(\vec{v}(X)) \cup X(B_M)$$

where the part $X(B_M)$ of $\partial C_2(M)$ is the graph of the restriction of the combing X to B_M and a *propagator associated with the combing* X is a 4–chain $\mathcal{P}_X$ of $C_2(M)$ whose boundary reads $\partial\mathcal{P}_X$. Such a $\mathcal{P}_X$ is indeed a propagator (because for a tiny sphere $\partial B(x)$ around a point x, $\langle x \times \partial B(x), \mathcal{P}_X\rangle_{C_2(M)}$ is the algebraic intersection in $U\check{M}$ of a fiber and the section $X(\check{M})$, which is one).

2.3 On the Θ-invariant of a combed $\mathbb{Q}$–sphere

Theorem 2.1 *Let X be a combing of a rational homology sphere M, and let $(-X)$ be the opposite combing. Let $\mathcal{P}_X$ and $\mathcal{P}_{-X}$ be two associated transverse propagators. Then $\mathcal{P}_X \cap \mathcal{P}_{-X}$ is a two-dimensional cycle whose homology class is independent of the chosen propagators. It reads $\Theta(M,X)[S]$, where $\Theta(M,X)$ is therefore a rational valued topological invariant of M and of the homotopy class of X.*

PROOF: Let us first show that $C_2(M)$ has the same rational homology as S^2. The space $C_2(M)$ is homotopy equivalent to $(\check{M}^2 \setminus \text{diag})$. Since $\check{M}$ is a rational homology

$\mathbb{R}^3$, the rational homology of $(\check{M}^2 \setminus \text{diag})$ is isomorphic to the rational homology of $((\mathbb{R}^3)^2 \setminus \text{diag})$. Since $((\mathbb{R}^3)^2 \setminus \text{diag})$ is homeomorphic to $\mathbb{R}^3 \times]0,\infty[\times S^2$ via the map

$$(x,y) \mapsto (x, \parallel y-x \parallel, \frac{1}{\parallel y-x \parallel}(y-x)),$$

$((\mathbb{R}^3)^2 \setminus \text{diag})$ is homotopy equivalent to S^2.

In particular, since $H_3(C_2(M);\mathbb{Q}) = 0$, there exist propagators $\mathcal{P}_X$ and $\mathcal{P}_{-X}$ with the given boundaries $\partial\mathcal{P}_X$ and $\partial\mathcal{P}_{-X}$. By general position arguments [4, Chapter 3], $\mathcal{P}_X$ and $\mathcal{P}_{-X}$ can be assumed to be transverse. (Explicit transverse propagators will be constructed in Subsections 6.2 and 6.3.) Without loss, assume that $\mathcal{P}_{\pm X} \cap \partial C_2(M) = \partial\mathcal{P}_{\pm X}$. Since $\partial\mathcal{P}_X$ and $\partial\mathcal{P}_{-X}$ do not intersect, $\mathcal{P}_X \cap \mathcal{P}_{-X}$ is a 2–cycle. Since $H_4(C_2(M);\mathbb{Q}) = 0$, the homology class of $\mathcal{P}_X \cap \mathcal{P}_{-X}$ in $H_2(C_2(M);\mathbb{Q})$ does not depend on the choices of $\mathcal{P}_X$ and $\mathcal{P}_{-X}$ with their given boundaries. Then it is easy to see that $\Theta(M,X) \in \mathbb{Q}$ is a locally constant function of the combing X. $\diamond$

When M is an integer homology sphere, a combing X is the first vector of a unique parallelization $\tau(X)$ that coincides with τ_s outside B_M, up to homotopy. When M is a rational homology sphere, and when X is the first vector of a such a parallelization $\tau(X)$, this parallelization is again unique. In this case, the invariant $\Theta(M,X)$ can be identified with the invariant $\Theta(M,\tau(X))$ discussed in Subsection 1.1 using [11, Lemma 6.16].

Let W be a connected compact 4–dimensional manifold with corners with signature 0 whose boundary is

$$\partial W = B_M \cup_{1\times\partial B_M} (-[0,1] \times S^2) \cup_{0\times S^2} (-B^3)$$

and that is identified with an open subspace of one of the products $[0,1[\times B^3$ or $]0,1] \times B_M$ near ∂W. Then the Pontrjagin number $p_1(\tau(X))$ is the obstruction to extending the trivialization of $TW \otimes \mathbb{C}$ induced by $\tau(X)$ and τ_s on ∂W to W. This obstruction lives in $H^4(W,\partial W;\pi_3(SU(4)) = \mathbb{Z}) = \mathbb{Z}$. See [10, Section 1.5] for more details. In [8], G. Kuperberg and D. Thurston proved that

$$\Theta(M,X) = 6\lambda(M) + \frac{p_1(\tau(X))}{4}$$

when M is an integer homology sphere. This result was extended to $\mathbb{Q}$–spheres by the author in [11, Theorem 2.6 and Section 6.5]. Setting $p_1(X) = (4\Theta(M,X) - 24\lambda(M))$ extends the Pontrjagin number from parallelizations to combings so that the formula above is still valid for combings.

The following theorem is proved in [13].

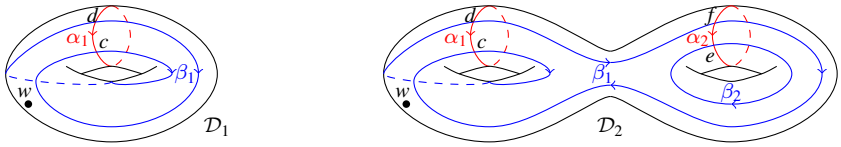

Figure 1: Two Heegaard diagrams of $\mathbb{RP}^3$

Theorem 2.2 *Let X and Y be two combings of M such that the cycle $\partial\mathcal{P}_Y$ is transverse to $\partial\mathcal{P}_X$ and to $\partial\mathcal{P}_{-X}$ in $\partial C_2(M)$. Then the oriented intersection $\partial\mathcal{P}_X \cap \partial\mathcal{P}_Y$ (resp. $\partial\mathcal{P}_X \cap \partial\mathcal{P}_{-Y}$) is the graph of the restriction of X to an oriented link $L_{X=Y}$ (resp. $L_{X=-Y}$) in $U\check{M}$ and*

$$\Theta(M,Y) - \Theta(M,X) = \frac{p_1(Y) - p_1(X)}{4} = lk(L_{X=Y}, L_{X=-Y}).$$

3 The formula for the Θ-invariant from Heegaard diagrams

3.1 On Heegaard diagrams

Every closed 3–manifold M can be written as the union of two handlebodies $H_{\mathcal{A}}$ and $H_{\mathcal{B}}$ glued along their common boundary, which is a genus g surface as

$$M = H_{\mathcal{A}} \cup_{\partial H_{\mathcal{A}}} H_{\mathcal{B}}$$

where $\partial H_{\mathcal{A}} = -\partial H_{\mathcal{B}}$. Such a decomposition is called a *Heegaard decomposition* or a *Heegaard splitting* of M. A *system of meridian disks* for $H_{\mathcal{A}}$ is a system of g disjoint disks $D(\alpha_i)$ properly embedded in $H_{\mathcal{A}}$ such that the union of the boundaries α_i of the $D(\alpha_i)$ does not separate $\partial H_{\mathcal{A}}$. Let $(D(\alpha_i))_{i\in\{1,\dots,g\}}$ be such a system for $H_{\mathcal{A}}$ and let $(D(\beta_j))_{j\in\{1,\dots,g\}}$ be such a system for $H_{\mathcal{B}}$. Then the surface equipped with the collections of the curves α_i and the curves $\beta_j = \partial D(\beta_j)$ determines M. When the collections $(\alpha_i)_{i\in\{1,\dots,g\}}$ and $(\beta_j)_{j\in\{1,\dots,g\}}$ are transverse, the data collection

$$\mathcal{D} = (\partial H_{\mathcal{A}}, (\alpha_i)_{i\in\{1,\dots,g\}}, (\beta_j)_{j\in\{1,\dots,g\}})$$

is called a *genus g Heegaard diagram.* Figure 1 shows two Heegaard diagrams of $\mathbb{RP}^3$ (or $SO(3)$).

We fix a genus g Heegaard diagram $\mathcal{D}$. A *crossing* c of $\mathcal{D}$ is an intersection point of a curve $\alpha_{i(c)}$ and a curve $\beta_{j(c)}$. Its sign $\sigma(c)$ is 1 if $\partial H_{\mathcal{A}}$ is oriented by the oriented tangent vector of $\alpha_{i(c)}$ followed by the oriented tangent vector of $\beta_{j(c)}$ at c. It is (-1) otherwise. The collection of crossings of $\mathcal{D}$ is denoted by $\mathcal{C}$.

Fix a point a_i inside each disk $D(\alpha_i)$ and a point b_j inside each disk $D(\beta_j)$. Then join a_i to each crossing c of α_i by a segment $[a_i, c]_{D(\alpha_i)}$ oriented from a_i to c in $D(\alpha_i)$, so that these segments only meet at a_i for different c. Similarly define segments $[c, b_{j(c)}]_{D(\beta_{j(c)})}$ from c to $b_{j(c)}$ in $D(\beta_{j(c)})$. Then for each c, define the *flow line* $\gamma(c) = [a_{i(c)}, c]_{D(\alpha_{i(c)})} \cup [c, b_{j(c)}]_{D(\beta_{j(c)})}$.

A Heegaard decomposition as above can be obtained from a Morse function f_M on M with one minimum, one maximum, index one-critical points a_i mapped to 1 and index 2 critical points b_j mapped to 5, by setting $H_{\mathcal{A}} = f_M^{-1}(]-\infty, 3])$ and $H_{\mathcal{B}} = f_M^{-1}([3, +\infty[)$ [4, Chapter 6]. For an appropriate (generic) metric, the descending manifolds of the b_j intersect $H_{\mathcal{B}}$ as disks $D(\beta_j)$ and the ascending manifolds of the a_i intersect $H_{\mathcal{A}}$ as disks $D(\alpha_i)$ so that the boundaries α_i of the $D(\alpha_i)$ are transverse to the boundaries β_j of the $D(\beta_j)$. The Morse function f_M and such a metric $\mathfrak{g}$ induce a Heegaard diagram of M where the flow line $\gamma(c)$ above can be chosen as the closure of the actual flow line through c for the gradient flow of f_M. Conversely, for any Heegaard diagram, there exist a Morse function and a metric as above that produce this diagram.

An *exterior point* of the diagram is a point of $\partial H_{\mathcal{A}} \setminus \left(\coprod_{i=1}^{g} \alpha_i \cup \coprod_{j=1}^{g} \beta_j\right)$ as in Figure 1. Pick an exterior point w of the diagram, and let $\overline{\gamma(w)}$ be the closure of the flow line through w with respect to $\mathfrak{g}$. It goes from the minimum of f_M to its maximum. Identify a ball around $\overline{\gamma(w)}$ with a neighborhood of ∞ in S^3, so that the restriction of f_M to B_M extends to $\check{M}$ as a Morse function f that is the standard height function outside B_M, that has no extremum, whose index one critical points a_i are mapped to 1, and whose index 2 critical points b_j are mapped to 5.

In Section 4, we describe an explicit propagator $\mathcal{P}(f, \mathfrak{g})$ associated with a Morse function f of $\check{M}$ that satisfies these properties, and with a metric $\mathfrak{g}$ that is standard outside B_M.

A *matching* in a genus g Heegaard diagram $(\partial H_{\mathcal{A}}, \{\alpha_i\}_{i=1,\dots,g}, \{\beta_j\}_{j=1,\dots,g})$ is a set $\mathfrak{m}$ of g crossings such that every curve of the diagram contains one crossing of $\mathfrak{m}$. Thus a matching $\mathfrak{m}$ can be written as $\mathfrak{m} = \{c_i; i \in \{1, 2, \dots, g\}\}$ where the c_i are crossings of $\alpha_i \cap \beta_{\rho^{-1}(i)}$ for a permutation ρ of $\{1, 2, \dots, g\}$.

The choice of a matching $\mathfrak{m}$ and of an exterior point w in a diagram $\mathcal{D}$ of M equips $\check{M}$ with a combing $X(w, \mathfrak{m}) = X(\mathcal{D}, w, \mathfrak{m})$, which is roughly obtained from the gradient vector of f by reversing this singular field along the flow lines through the points of $\mathfrak{m}$. The combing $X(w, \mathfrak{m})$ of $\check{M}$ is precisely described in Subsection 5.1. [1] The propagator

[1] The same data $(\mathcal{D}, w, \mathfrak{m})$ can be used to define an Euler structure or a combing of the non-punctured M. Such a combing represents a Spin^c structure. Matchings representing a given

$\mathcal{P}(f,\mathfrak{g})$ is modified near $\partial C_2(M)$ to become a propagator $\mathcal{P}_{X(w,\mathfrak{m})}$ associated with $X(w,\mathfrak{m})$ in Subsection 5.2.

Sections 6 and 7 are devoted to the computation of $\Theta(M,X(w,\mathfrak{m}))$, performed by evaluating the homology class of the intersection of $\mathcal{P}_{X(w,\mathfrak{m})}$ and $\mathcal{P}_{-X(w,\mathfrak{m})}$, and by applying the definition of Theorem 2.1. The current section is devoted to presenting the combinatorial formula

$$\Theta(M,X(\mathcal{D},w,\mathfrak{m})) = \ell_2(\mathcal{D}) + lk(L(\mathcal{D},\mathfrak{m}),L(\mathcal{D},\mathfrak{m})_{\|}) - e(\mathcal{D},w,\mathfrak{m})$$

that we get from our computation.

The three ingredients of our formula are completely combinatorial. They can be read on the Heegaard diagram without referring to Morse functions. However, they also have a topological meaning, which explains the chosen notation and which makes them easier to apprehend. We first introduce the ingredients $lk(L(\mathcal{D},\mathfrak{m}),L(\mathcal{D},\mathfrak{m})_{\|})$ and $\ell_2(\mathcal{D})$ with their topological interpretations in Subsections 3.2 and 3.3, respectively, before giving their combinatorial expressions in Corollary 3.5 at the end of Subsection 3.4. The combinatorial definition of $e(\mathcal{D},w,\mathfrak{m})$ is given in Subsection 3.5.

Let

$$[\mathcal{J}_{ji}]_{(j,i)\in\{1,\dots,g\}^2} = [\langle\alpha_i,\beta_j\rangle_{\partial H_{\mathcal{A}}}]^{-1}$$

be the inverse matrix of the matrix of the algebraic intersection numbers $\langle\alpha_i,\beta_j\rangle_{\partial H_{\mathcal{A}}}$.

$$\sum_{i=1}^{g}\mathcal{J}_{ji}\langle\alpha_i,\beta_k\rangle_{\partial H_{\mathcal{A}}} = \delta_{jk} = \begin{cases} 1 & \text{if } j=k \\ 0 & \text{otherwise.}\end{cases}$$

Let

$$L(\mathfrak{m}) = L(\mathcal{D},\mathfrak{m}) = \sum_{i=1}^{g}\gamma(c_i) - \sum_{c\in\mathcal{C}}\mathcal{J}_{j(c)i(c)}\sigma(c)\gamma(c).$$

Note that $L(\mathfrak{m})$ is a cycle since

$$\partial L(\mathfrak{m}) = \sum_{i=1}^{g}(b_i-a_i) - \sum_{(i,j)\in\{1,\dots,g\}^2}\mathcal{J}_{ji}\langle\alpha_i,\beta_j\rangle_{\partial H_{\mathcal{A}}}(b_j-a_i) = 0.$$

The term $lk(L(\mathcal{D},\mathfrak{m}),L(\mathcal{D},\mathfrak{m})_{\|})$ is the linking number of $L(\mathfrak{m})$ with a canonical parallel $L(\mathfrak{m})_{\|}$ of $L(\mathfrak{m})$ that is defined in Subsection 3.2 below.

Spin^c-structure ξ are the generators of a chain complex whose homology is a Heegaard-Floer homology of (M,ξ).

Example 3.1 For the genus one Heegaard diagram $\mathcal{D}_1$ of Figure 1, $\sigma(c) = 1$, $\langle \alpha_1, \beta_1 \rangle_{\partial H_{\mathcal{A}}} = 2$, $\mathcal{J}_{11} = \frac{1}{2}$, we choose $\{c\}$ as a matching and $L(\{c\}) = \frac{1}{2}(\gamma(c) - \gamma(d))$.

For the genus two Heegaard diagram $\mathcal{D}_2$ of Figure 1, $\langle \alpha_2, \beta_1 \rangle_{\partial H_{\mathcal{A}}} = 1$, $\mathcal{J}_{11} = \frac{1}{2}$, $\mathcal{J}_{22} = 1$, $\mathcal{J}_{12} = 0$, $\mathcal{J}_{21} = -\frac{1}{2}$, we choose the matching $\{c, e\}$ and $L(\{c, e\}) = \frac{1}{2}(\gamma(c) - \gamma(d))$.

3.2 Parallels of flow lines

For a crossing $c \in \alpha_{i(c)} \cap \beta_{j(c)}$, $\gamma(c)_{\|}$ will denote the following chain. Consider a small meridian curve $m(c)$ of $\gamma(c)$ on $\partial H_{\mathcal{A}}$, it intersects $\beta_{j(c)}$ at two points: $c^+_{\mathcal{A}}$ on the positive side of $D(\alpha_{i(c)})$ and $c^-_{\mathcal{A}}$ on the negative side of $D(\alpha_{i(c)})$. The meridian $m(c)$ also intersects $\alpha_{i(c)}$ at $c^+_{\mathcal{B}}$ on the positive side of $D(\beta_{j(c)})$ and $c^-_{\mathcal{B}}$ on the negative side of $D(\beta_{j(c)})$. Let $[c^+_{\mathcal{A}}, c^+_{\mathcal{B}}]$, $[c^+_{\mathcal{A}}, c^-_{\mathcal{B}}]$, $[c^-_{\mathcal{A}}, c^+_{\mathcal{B}}]$ and $[c^-_{\mathcal{A}}, c^-_{\mathcal{B}}]$ denote the four quarters of $m(c)$ with the natural ends and orientations associated with the notation, as in Figure 2.

Figure 2: $m(c)$, $c^+_{\mathcal{A}}$, $c^-_{\mathcal{A}}$, $c^+_{\mathcal{B}}$ and $c^-_{\mathcal{B}}$

For each point a_i, choose a point a_i^+ and a point a_i^- close to a_i outside $D(\alpha_i)$ so that a_i^+ is on the positive side of $D(\alpha_i)$ (the side of the positive normal) and a_i^- is on the negative side of $D(\alpha_i)$. Similarly fix points b_j^+ and b_j^- close to the b_j and outside the $D(\beta_j)$.

Let $\gamma^+_{\mathcal{A}}(c)$ (resp. $\gamma^-_{\mathcal{A}}(c)$) be an arc parallel to $[a_{i(c)}, c]_{D(\alpha_{i(c)})}$ from $a^+_{i(c)}$ to $c^+_{\mathcal{A}}$ (resp. from $a^-_{i(c)}$ to $c^-_{\mathcal{A}}$) that does not meet $D(\alpha_{i(c)})$. Let $\gamma^+_{\mathcal{B}}(c)$ (resp. $\gamma^-_{\mathcal{B}}(c)$) be an arc parallel to $[c, b_{j(c)}]_{D(\beta_{j(c)})}$ from $c^+_{\mathcal{B}}$ to $b^+_{j(c)}$ (resp. from $c^-_{\mathcal{B}}$ to $b^-_{j(c)}$) that does not meet $D(\beta_{j(c)})$.

$$\begin{aligned}\gamma(c)_{\|} = \ & \tfrac{1}{2}(\gamma^+_{\mathcal{A}}(c) + \gamma^-_{\mathcal{A}}(c)) + \tfrac{1}{2}(\gamma^+_{\mathcal{B}}(c) + \gamma^-_{\mathcal{B}}(c)) \\ & + \tfrac{1}{4}([c^+_{\mathcal{A}}, c^+_{\mathcal{B}}] + [c^+_{\mathcal{A}}, c^-_{\mathcal{B}}] + [c^-_{\mathcal{A}}, c^+_{\mathcal{B}}] + [c^-_{\mathcal{A}}, c^-_{\mathcal{B}}]).\end{aligned}$$

Since the $+$ and the $-$ play the same roles in the above formula, $\gamma(c)_{\|}$ does not depend on the orientations of the α_i and the β_j. Set $a_{i\|} = \frac{1}{2}(a_i^+ + a_i^-)$ and $b_{j\|} = \frac{1}{2}(b_j^+ + b_j^-)$. Then $\partial\gamma(c)_{\|} = b_{j(c)\|} - a_{i(c)\|}$.

Set $L(\mathfrak{m})_{\|} = \sum_{i=1}^{g} \gamma(c_i)_{\|} - \sum_{c\in\mathcal{C}} \mathcal{J}_{j(c)i(c)}\sigma(c)\gamma(c)_{\|}$ and note that $L(\mathfrak{m})_{\|}$ is a cycle disjoint from $L(\mathfrak{m})$. The cycle $L(\mathfrak{m})$ depends neither on the orientations of the α_i and the β_j, nor on their order. Permuting the roles of the α_i and the roles of the β_j reverses the orientations of $L(\mathfrak{m})$ and $L(\mathfrak{m})_{\|}$ and leaves $lk(L(\mathfrak{m}), L(\mathfrak{m})_{\|})$ unchanged.

3.3 A 2-cycle $G(\mathcal{D})$ of $C_2(M)$ associated with a Heegaard diagram

The term $\ell_2(\mathcal{D})$ will be defined from the homology class of the 2–cycle $G(\mathcal{D})$ of $C_2(M)$ associated with the Heegaard diagram in the following proposition 3.2, by the equality $[G(\mathcal{D})] = \ell_2(\mathcal{D})[S]$ in $H_2(C_2(M);\mathbb{Q})$. This term $\ell_2(\mathcal{D})$ can be thought of as the main term of the formula, the other ones can be thought of as correction terms.

Proposition 3.2 *Set*

$$G(\mathcal{D}) = \sum_{(c,d)\in\mathcal{C}^2} \mathcal{J}_{j(c)i(d)}\mathcal{J}_{j(d)i(c)}\sigma(c)\sigma(d)(\gamma(c)\times\gamma(d)_{\|}) - \sum_{c\in\mathcal{C}} \mathcal{J}_{j(c)i(c)}\sigma(c)(\gamma(c)\times\gamma(c)_{\|}).$$

Then $G(\mathcal{D})$ is a 2–cycle of $C_2(M)$. Its homology class $[G(\mathcal{D})]$ depends neither on the orientations of the α_i and the β_j, nor on their order. Permuting the roles of the α_i and the roles of the β_j does not change it either.

PROOF: Let us first prove that $G(\mathcal{D})$ is a 2-cycle. Let $d\in\mathcal{C}$. For any j,

$$\sum_{c\in\beta_j} \mathcal{J}_{j(d)i(c)}\sigma(c) = \sum_{i=1}^{g} \mathcal{J}_{j(d)i}\langle\alpha_i,\beta_j\rangle = \delta_{jj(d)}$$

and, for any i, $\sum_{c\in\alpha_i} \mathcal{J}_{j(c)i(d)}\sigma(c) = \sum_{j=1}^{g} \mathcal{J}_{ji(d)}\langle\alpha_i,\beta_j\rangle = \delta_{ii(d)}$. Therefore, for any $d\in\mathcal{C}$,

$$\partial\left(\sum_{c\in\mathcal{C}} \mathcal{J}_{j(c)i(d)}\mathcal{J}_{j(d)i(c)}\sigma(c)\gamma(c)\right) = \mathcal{J}_{j(d)i(d)}(b_{j(d)} - a_{i(d)}) = \mathcal{J}_{j(d)i(d)}\partial\gamma(d)$$

and

$$\begin{aligned}\partial G(\mathcal{D}) &= \textstyle\sum_{d\in\mathcal{C}} \sigma(d)\mathcal{J}_{j(d)i(d)}(\partial\gamma(d))\times\gamma(d)_{\|} - \sum_{c\in\mathcal{C}} \mathcal{J}_{j(c)i(c)}\sigma(c)(\partial\gamma(c))\times\gamma(c)_{\|}\\ &\quad \textstyle- \sum_{c\in\mathcal{C}} \mathcal{J}_{j(c)i(c)}\sigma(c)\gamma(c)\times\partial\gamma(c)_{\|} + \sum_{c\in\mathcal{C}} \mathcal{J}_{j(c)i(c)}\sigma(c)\gamma(c)\times\partial\gamma(c)_{\|}\\ &= 0.\end{aligned}$$

Since changing the orientation of $\alpha_{i(c)}$ leaves $\mathcal{J}_{j(d)i(c)}\sigma(c)$ invariant and changing the orientation of $\beta_{j(c)}$ leaves $\mathcal{J}_{j(c)i(d)}\sigma(c)$ invariant, the cycle $G(\mathcal{D})$ does not depend on the orientations of the α_i and the β_j. It clearly does not depend on the numbering. It is also easy to see that permuting the roles of the α_i and the β_j reverses the orientations

of the $\gamma(c)$, changes $\mathcal{J}$ to the transposed matrix and does not change the cycle $G(\mathcal{D})$ either. $\diamond$

Note that $\ell_2(\mathcal{D})$ is additive under connected sum of Heegaard diagrams, and therefore it is invariant under stabilisation of diagrams, but, as Example 3.9 will show, it is not an invariant of Heegaard splittings. In the next subsection, we state Proposition 3.4 that yields combinatorial formulae both for $\ell_2(\mathcal{D})$ and for $lk(L(\mathcal{D},\mathfrak{m}),L(\mathcal{D},\mathfrak{m})_{\|})$.

3.4 Evaluating some 2–cycles of $C_2(M)$

When d and e are (possibly equal) crossings of α_i, $[d,e]_{\alpha_i}=[d,e]_\alpha$ denotes the set of crossings from d to e (including them) along α_i, or the closed arc from d to e in α_i depending on the context. Then $[d,e[_\alpha = [d,e]_\alpha \setminus \{e\}$.

Now, for such a part I of α_i,

$$\langle I,\beta_j\rangle = \sum_{c\in I\cap\beta_j}\sigma(c).$$

We shall also use the notation $|$ for ends of arcs to say that an end is "half-contained" in an arc, and that it must be counted with coefficient $1/2$. ("$[d,e|_\alpha=[d,e]_\alpha\setminus\{e\}/2$" and "$|d,e|_\alpha=[d,e|_\alpha\setminus\{d\}/2$" so that $|d,d|_\alpha=\emptyset$.)

We use the same notation for arcs $[d,e|_{\beta_j}=[d,e|_\beta$ of β_j. For example, if d is a crossing of $\alpha_i\cap\beta_j$, then

$$\langle [d,d|_\alpha,\beta_j\rangle = \frac{\sigma(d)}{2}$$

and

$$\langle [c,d|_\alpha,[e,d|_\beta\rangle = \frac{\sigma(d)}{4}+\sum_{c\in[c,d[_\alpha\cap[e,d[_\beta}\sigma(c).$$

Example 3.3 In the diagram $\mathcal{D}_1$ of Figure 1, $\langle [c,c|_\alpha,[c,c|_\beta\rangle=\frac14$, $\langle [c,c|_\alpha,[c,d|_\beta\rangle = \langle [c,d|_\alpha,[c,c|_\beta\rangle=\frac12$, $\langle [c,d|_\alpha,[c,d|_\beta\rangle=\frac54$, $\langle [c,c|_\alpha,\beta_1\rangle=\frac12$ and $\langle [c,d|_\alpha,\beta_1\rangle=\frac32$.

The following proposition is proved in Subsection 4.3.

Proposition 3.4 *For every curve α_i (resp. β_j), choose a basepoint $p(\alpha_i)$ (resp. $p(\beta_j)$). These choices being made, for two crossings c and d of $\mathcal{C}$, set*

$$\begin{aligned}\ell(c,d) = {}& \langle [p(\alpha(c)),c|_\alpha,[p(\beta(d)),d|_\beta\rangle\\ & -\textstyle\sum_{(i,j)\in\{1,\dots,g\}^2}\mathcal{J}_{ji}\langle [p(\alpha(c)),c|_\alpha,\beta_j\rangle\langle\alpha_i,[p(\beta(d)),d|_\beta\rangle\end{aligned}$$

where $\alpha(c)=\alpha_{i(c)}$ and $\beta(c)=\beta_{j(c)}$. Then, for any 2–cycle $G=\sum_{(c,d)\in\mathcal{C}^2} g_{cd}(\gamma(c)\times\gamma(d)_{\|})$ of $C_2(M)$,

$$[G]=\sum_{(c,d)\in\mathcal{C}^2} g_{cd}\ell(c,d)[S]=\sum_{(c,d)\in\mathcal{C}^2} g_{cd}\ell(d,c)[S].$$

We have the following immediate corollary of Proposition 3.4.

Corollary 3.5 *For any choice of ℓ as in Proposition 3.4*

$$\ell_2(\mathcal{D})=\sum_{(c,d)\in\mathcal{C}^2}\mathcal{J}_{j(c)i(d)}\mathcal{J}_{j(d)i(c)}\sigma(c)\sigma(d)\ell(c,d)-\sum_{c\in\mathcal{C}}\mathcal{J}_{j(c)i(c)}\sigma(c)\ell(c,c)$$

and

$$\begin{aligned} lk(L(\mathcal{D},\mathfrak{m}),L(\mathcal{D},\mathfrak{m})_{\|})= &\ \textstyle\sum_{(i,j)\in\{1,\dots,g\}^2}\ell(c_i,c_j)\\ &+\textstyle\sum_{(c,d)\in\mathcal{C}^2}\mathcal{J}_{j(c)i(c)}\mathcal{J}_{j(d)i(d)}\sigma(c)\sigma(d)\ell(c,d)\\ &-\textstyle\sum_{(i,c)\in\{1,\dots,g\}\times\mathcal{C}}\mathcal{J}_{j(c)i(c)}\sigma(c)(\ell(c_i,c)+\ell(c,c_i)).\end{aligned}$$

PROOF: Recall $[L(\mathfrak{m})\times L(\mathfrak{m})_{\|}]=lk(L(\mathfrak{m}),L(\mathfrak{m})_{\|})[S]$ in $H_2(C_2(M);\mathbb{Q})$. ◇

Example 3.6 Again, consider the diagram $\mathcal{D}_1$ of Figure 1. Choose $p(\alpha_1)=p(\beta_1)=c$. Using Example 3.3, we get

$$\ell(c,c)=\frac{1}{4}-\frac{1}{8}=\frac{1}{8},\ell(d,d)=\frac{5}{4}-\frac{9}{8}=\frac{1}{8},\ell(c,d)=\ell(d,c)=\frac{1}{2}-\frac{3}{8}=\frac{1}{8}.$$

For the diagram $\mathcal{D}_2$ of Figure 1, choose $p(\alpha_1)=p(\beta_1)=c$ and $p(\alpha_2)=p(\beta_2)=e$. Then we still have $\ell(c,c)=\ell(c,d)=\ell(d,c)=\ell(d,d)=\frac{1}{8}$. Furthermore, $\ell(e,e)=0$, and, as a nonsymmetric example, $\ell(c,e)=0$ and $\ell(e,c)=\frac{1}{8}$. Then $lk(L(\{c\}),L(\{c\})_{\|})=lk(L(\{c,e\}),L(\{c,e\})_{\|})=0$, and $\ell_2(\mathcal{D}_1)=\ell_2(\mathcal{D}_2)=0$.

3.5 Combinatorial definition of $e(w,\mathfrak{m})$

Recall that we fixed a matching $\mathfrak{m}=\{c_i;i\in\{1,2,\dots,g\}\}$ where the c_i are crossings of $\alpha_i\cap\beta_{\rho^{-1}(i)}$ for a permutation ρ of $\{1,2,\dots,g\}$. Select an exterior point w of $\mathcal{D}$. These choices being fixed, represent the Heegaard diagram $\mathcal{D}$ in a plane by removing a topological disk around w and by cutting the surface $\partial H_{\mathcal{A}}$ along the α_i. The boundary of the removed topological disk will be pictured as a rectangle, and each α_i gives rise to two boundary components of the planar surface, which are copies of α_i denoted by α_i' and α_i''. They are drawn as circles. The crossing c_i is located at the points with upward tangents of α_i' and α_i'', while the other crossings are located near the

points with downward tangents as in Figure 3. The curves β_j intersect this picture as families of arcs, which begin and end at crossings with the α_i' and the α_i'' where they are horizontal. A diagram with these properties is called a *rectangular diagram* of $(\mathcal{D}, \mathfrak{m}, w)$.

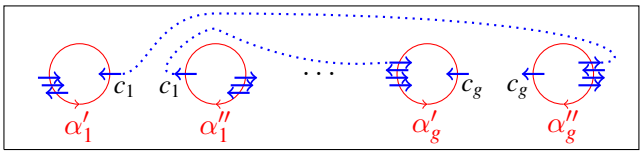

Figure 3: Rectangular diagram of $(\mathcal{D}, \mathfrak{m}, w)$

The rectangle has the standard parallelization of the plane. Then there is a map "unit tangent vector" from each partial projection of a beta curve β_j in the plane to S^1. The total degree of this map for the curve β_j is denoted by $d_e(\beta_j)$. For a crossing $c \in \beta_j$, $d_e(|c_{\rho(j)}, c|_\beta) \in \frac{1}{2}\mathbb{Z}$ denotes the degree of the restriction of this map to the arc $|c_{\rho(j)}, c|_\beta$. This degree is the average of the degrees of this map at the upward vertical vector and at the downward one. For every $c \in \mathcal{C}$, define

$$d_e(c) = d_e(|c_{\rho(j(c))}, c|_\beta) - \sum_{(r,s)\in\{1,\dots,g\}^2} \mathcal{J}_{sr}\langle \alpha_r, |c_{\rho(j(c))}, c|_\beta \rangle d_e(\beta_s),$$

where $|c, c|_\beta = \emptyset$. Then set

$$e(w, \mathfrak{m}) = e(\mathcal{D}, w, \mathfrak{m}) = \sum_{c\in\mathcal{C}} \mathcal{J}_{j(c)i(c)}\sigma(c)d_e(c).$$

In Section 7.1, $e(w, \mathfrak{m})$ will be identified with an Euler class. See Proposition 7.2.

Example 3.7 For the Heegaard diagram $\mathcal{D}_1$ equipped with the matching $\mathfrak{m} = \{c\}$, there are two choices for an exterior point w up to isotopy, the choice w of Figure 1, and the choice of a point w' in the other connected component of $\partial H_{\mathcal{A}} \setminus (\alpha_1 \cup \beta_1)$. These choices give rise to the two rectangular diagrams of $(\mathcal{D}_1, \mathfrak{m}, w)$ and $(\mathcal{D}_1, \mathfrak{m}, w')$ shown in Figure 4.

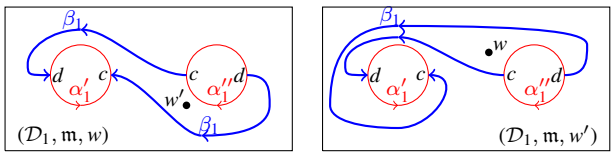

Figure 4: Rectangular diagrams of $(\mathcal{D}_1, \{c\}, w)$ and $(\mathcal{D}_1, \{c\}, w')$

For both rectangular diagrams, we have $d_e(|c,c|_\beta)=0$, $d_e(c)=0$ and $d_e(|c,d|_\beta)=\frac{1}{2}$ while $d_e(\beta_1)=0$ for $(\mathcal{D}_1,\{c\},w)$ and $d_e(\beta_1)=2$ for $(\mathcal{D}_1,\{c\},w')$ so that $d_e(d)=\frac{1}{2}$ for $(\mathcal{D}_1,\{c\},w)$ and $d_e(d)=-\frac{1}{2}$ for $(\mathcal{D}_1,\{c\},w')$. Thus $e(w',\{c\})=-\frac{1}{4}$ and $e(w,\{c\})=\frac{1}{4}$.

3.6 Statement of the main theorem

The main result of this article is the following theorem.

Theorem 3.8 *For any Heegaard diagram $\mathcal{D}$ of a rational homology sphere M, for any exterior point w of $\mathcal{D}$, and for any matching $\mathfrak{m}$ of $\mathcal{D}$,*

$$\Theta(M,X(\mathcal{D},w,\mathfrak{m}))=\ell_2(\mathcal{D})+lk(L(\mathcal{D},\mathfrak{m}),L(\mathcal{D},\mathfrak{m})_{\|})-e(\mathcal{D},w,\mathfrak{m}).$$

Example 3.9 According to the computations of Examples 3.6 and 3.7,

$$\Theta(\mathbb{RP}^3,X(w,\{c\}))=-\frac{1}{4}$$

and $\Theta(\mathbb{RP}^3,X(w',\{c\}))=\frac{1}{4}$. Since $\lambda(\mathbb{RP}^3)=0$, this implies that $p_1(X(w',\{c\}))=1$ and $p_1(X(w,\{c\}))=-1$.

Let us now evaluate the ingredients of our formula for the rectangular genus two diagram $(\mathcal{D}_2,\{c,e\},w)$ of Figure 5. Recall from Example 3.6 that $lk(L(\{c,e\}),L(\{c,e\})_{\|})=0$, and $\ell_2(\mathcal{D}_2)=0$ and observe $e(\mathcal{D}_2,w,\{c,e\})=\frac{1}{4}$ so that $\Theta(\mathbb{RP}^3,X(\mathcal{D}_2,w,\{c,e\}))=-\frac{1}{4}$.

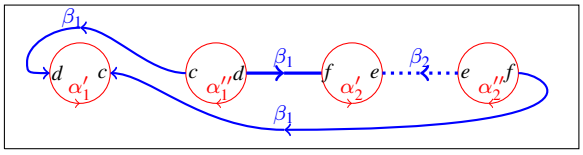

Figure 5: $(\mathcal{D}_2,\{c,e\},w)$

Consider the diagram $(\mathcal{D}_3,\{c,e\},w)$ of Figure 6 obtained from $(\mathcal{D}_2,\{c,e\},w)$ by an isotopy of β_2 on $\partial H_{\mathcal{A}}$. The $\mathcal{J}_{ji}$ are the same as for $\mathcal{D}_2$, and $L(\mathcal{D}_3,\{c,e\})=\frac{1}{2}(\gamma(c)-\gamma(d))+\frac{1}{2}(\gamma(g)-\gamma(h))$. Again, choosing $p(\alpha_1)=p(\beta_1)=c$ and $p(\alpha_2)=p(\beta_2)=e$, $\ell(c,c)=\ell(c,d)=\ell(d,c)=\ell(d,d)=\frac{1}{8}$ and $\ell(e,e)=0$. For any crossing $x\in\{c,d,e,f\}$, $\ell(g,x)=\ell(h,x)$ and $\ell(x,g)=\ell(x,h)$. Furthermore, $\ell(g,h)=\ell(h,g)$, $\ell(g,g)=\ell(h,g)+\frac{1}{4}$ and $\ell(h,h)=\ell(h,g)-\frac{1}{4}$ so that $lk(L(\mathcal{D}_3,\{c,e\}),L(\mathcal{D}_3,\{c,e\})_{\|})=$

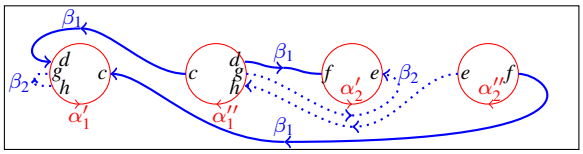

Figure 6: $(\mathcal{D}_3, \{c, e\}, w)$

0 and $\ell_2(\mathcal{D}_3) = \mathcal{J}_{21}(\ell(h,h) - \ell(g,g)) = \frac{1}{4}$. Thus $\ell_2(\mathcal{D})$ is not an invariant of Heegaard splittings. Since $d_e(g) = -\frac{1}{2}$, $e(\mathcal{D}_3, w, \{c, e\}) = \frac{1}{4} + \frac{1}{4} = \frac{1}{2}$. Again $\Theta(\mathbb{RP}^3, X(\mathcal{D}_3, w, \{c, e\})) = -\frac{1}{4}$.

A systematic study of the variations of the three ingredients of the formula under the moves that relate two Heegaard diagrams of a rational homology 3-sphere is performed in [14].

4 Propagators associated with Morse functions

In this section, we introduce a propagator $\mathcal{P}(f, \mathfrak{g})$ associated with a Morse function f without minima and maxima of $\check{M}$, and with a metric $\mathfrak{g}$ that is standard outside B_M. This Morse propagator has been constructed in a joint work with Greg Kuperberg. The pair $(f, \mathfrak{g})$ is supposed to give rise to the Heegaard diagram $\mathcal{D}$ of Section 3 as in Subsection 3.1.

We use the propagator $\mathcal{P}(f, \mathfrak{g})$ (whose boundary is not associated with a combing) to prove Proposition 3.4. Similar propagators associated with more general Morse functions have been constructed by Watanabe in [17], independently.

4.1 The Morse function f

Start with $\mathbb{R}^3$ equipped with its standard height function f_0 and replace the parallelepiped $[0, 2g] \times [0, 4] \times [0, 6]$ with a rational homology cube C_M (which has the rational homology of a point) equipped with a Morse function f that coincides with f_0 on $\partial([0, 2g] \times [0, 4] \times [0, 6])$, and that has $2g$ critical points, g points $a_1, \dots, a_g$ of index 1, which are mapped to 1 by f, and g points $b_1, \dots, b_g$ of index 2, which are mapped to 5 by f. Let $\check{M}$ be the associated open manifold, and let M be its one-point compactification. Equip $\check{M}$ with a Riemannian metric $\mathfrak{g}$ that coincides with the standard one outside $[0, 2g] \times [0, 4] \times [0, 6]$.

The preimage H_a of $]-\infty,2]$ under f in C_M has the standard representation of the bottom part of Figure 7. Our standard representation of the preimage H_b of $[4,+\infty[$ under f in C_M is shown in the upper part of Figure 7. It can be thought of as the complement of the bottom part in $[0,2g]\times[0,4]\times[0,6]$.

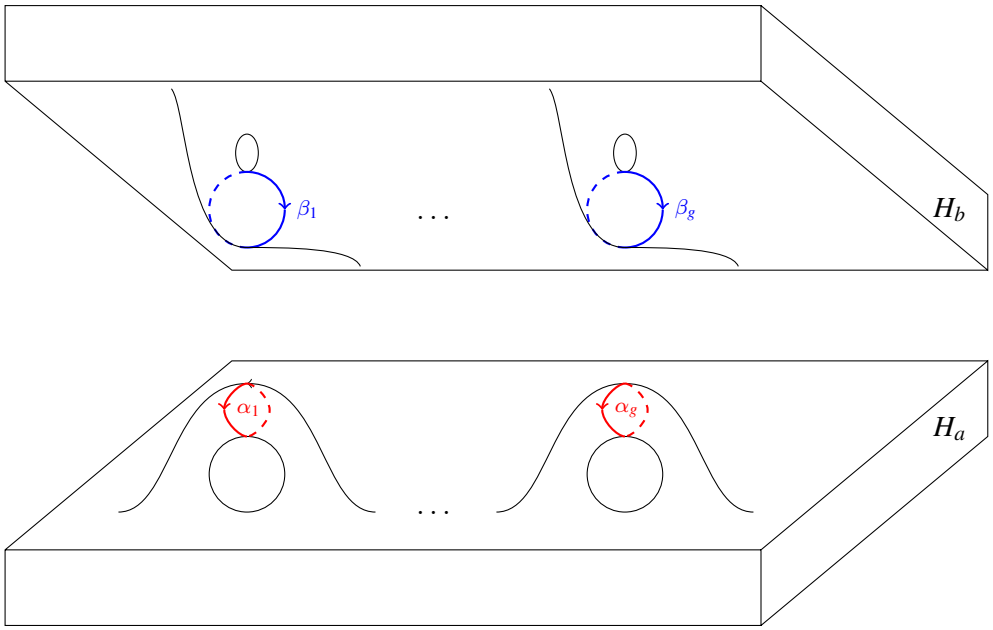

Figure 7: H_a and H_b

The two-dimensional ascending manifold of a_i is oriented arbitrarily, its closure is denoted by $\mathcal{A}_i$. Its intersection with H_a is denoted by $D(\alpha_i)$. The boundary of $D(\alpha_i)$ is denoted by α_i. The descending manifold of a_i is made of two half-lines $\mathcal{L}_+(a_i)$ and $\mathcal{L}_-(a_i)$ starting as vertical lines and ending at a_i. The one with the orientation of the positive normal to $\mathcal{A}_i$ is called $\mathcal{L}_+(a_i)$. Thus $\mathcal{L}(a_i)=\mathcal{L}_+(a_i)\cup(-\mathcal{L}_-(a_i))$ is the descending manifold of a_i.

Symmetrically, the two-dimensional descending manifold of b_j is oriented arbitrarily, its closure is denoted by $\mathcal{B}_j$. The $\mathcal{B}_j$ are assumed to be transverse to the $\mathcal{A}_i$ outside the critical points. The ascending manifold of b_j is made of two half-lines $\mathcal{L}_+(b_j)$ and $\mathcal{L}_-(b_j)$ starting at b_j and ending as vertical lines. The one with the orientation of the positive normal to $\mathcal{B}_j$ is called $\mathcal{L}_+(b_j)$. Thus $\mathcal{L}(b_j)=\mathcal{L}_+(b_j)-\mathcal{L}_-(b_j)$ is the ascending manifold of b_j. See Figure 8.

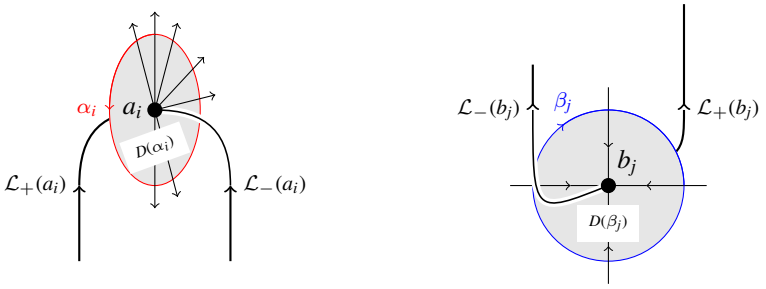

Figure 8: $\mathcal{L}_+(a_i)$, $\mathcal{L}_-(a_i)$, $\mathcal{L}_+(b_j)$, $\mathcal{L}_-(b_j)$

Let

$$H_{a,2} = C_M \cap f^{-1}(2)$$

and similarly define $H_{b,4} = C_M \cap f^{-1}(4)$. The preimage of $[2,4]$ in C_M is the product $H_{a,2} \times [2,4]$. Its intersection with $\mathcal{A}_i$ is $-\alpha_i \times [2,4]$ and its intersection with $\mathcal{B}_j$ is $\beta_j \times [2,4]$. Each crossing c of $\alpha_i \cap \beta_j$ has a sign $\sigma(c)$ and an associated flow line $\gamma(c)$ from a_i to b_j oriented as such.

Note the following lemma.

Lemma 4.1 *Let $c \in \alpha_i \cap \beta_j$. Along $\gamma(c)$, $\mathcal{A}_i$ is cooriented by $\sigma(c)\beta_j$ and $\mathcal{B}_j$ is cooriented by $\sigma(c)\alpha_i$.*

$$\mathcal{B}_j \cap \mathcal{A}_i = \sum_{c \in \alpha_i \cap \beta_j} \sigma(c)\gamma(c).$$

◇

4.2 The propagator $\mathcal{P}(f, \mathfrak{g})$

Let $s_\phi(\check{M})$ be the closure in $U\check{M}$ of the (graph of the) section of $U\check{M}_{|\check{M}\setminus\{a_i,b_i;i\in\{1,\dots,g\}\}}$ directed by the gradient of f. This closure contains the restriction of the unit tangent bundle to the critical points, up to orientation. Let ϕ be the flow associated with the gradient of f. Let P_ϕ be the closure in $C_2(M)$ of the image of

$$\begin{array}{lll} \big(\check{M} \setminus \{a_i, b_i; i \in \{1,\dots,g\}\}\big) \times]0,+\infty[& \to & C_2(M) \\ (x,t) & \mapsto & (x, \phi_t(x)), \end{array}$$

let $\big((\mathcal{B}_j \times \mathcal{A}_i) \cap C_2(M)\big)$ denote the closure of $\big((\mathcal{B}_j \times \mathcal{A}_i) \cap (\check{M}^2 \setminus \text{diagonal})\big)$ in $C_2(M)$, set

$$P_{\mathcal{I}} = \sum_{(i,j)\in\{1,\dots,g\}^2} \mathcal{J}_{ji}\big((\mathcal{B}_j \times \mathcal{A}_i) \cap C_2(M)\big) \qquad \text{and} \qquad \mathcal{P}(f,\mathfrak{g}) = P_\phi + P_{\mathcal{I}}$$

Let $\vec{v}$ be the upward vector in S^2, and let

$$\partial_{od} = p_\infty^{-1}(\vec{v}) \cap \left(\partial C_2(M) \setminus U\check{M}\right)$$

be a boundary part *outside the diagonal of* $\check{M}^2$. (If $\vec{v}_\infty$ denotes the upward vertical vector in the boundary of the compactification $C_1(M)$ of $\check{M}$, then ∂_{od} contains $\left(-\check{M} \times \vec{v}_\infty - \left((-\vec{v}_\infty) \times \check{M}\right)\right)$.)

Theorem 4.2 (Kuperberg–Lescop) *The 4–chain $\mathcal{P}(f,\mathfrak{g})$ is a propagator and its boundary, which lies in $\partial C_2(M)$, is*

$$\partial\mathcal{P}(f,\mathfrak{g}) = \partial_{od} + \sum_{c\in\mathcal{C}} \mathcal{J}_{j(c)i(c)}\sigma(c)U\check{M}_{|\gamma(c)} + \overline{s_\phi(\check{M})}$$

where $\overline{s_\phi(\check{M})}$ is the closure of $s_\phi(\check{M})$ in $\partial C_2(M)$.

PROOF: The expression of $\partial\mathcal{P}(f,\mathfrak{g})$ is the immediate consequence of the following two lemmas. Then it is easy to see that, for a tiny sphere $\partial B(x)$ around a point x outside the $\gamma(c)$, $\langle (x\times\partial B(x)), \mathcal{P}(f,\mathfrak{g})\rangle_{C_2(M)}$ is the algebraic intersection in $U\check{M}$ of a fiber and the section $s_\phi(\check{M})$, which is one. ◇

Note that $U\check{M}_{|\gamma(c)}$ is diffeomorphic to $S^2\times\gamma(c)$. For simplicity, $U\check{M}_{|\gamma(c)}$ will sometimes be simply denoted by $S^2\times\gamma(c)$, or by $S^2\times_\tau\gamma(c)$ when the parallelization τ that induces such a diffeomorphism matters.

Lemma 4.3

$$\partial P_\phi = \partial_{od} + \overline{s_\phi(\check{M})} - \sum_{i=1}^{g} \mathcal{L}(a_i)\times\mathcal{A}_i - \sum_{j=1}^{g} \mathcal{B}_j\times\mathcal{L}(b_j)$$

PROOF: The boundary of P_ϕ is made of $\left(\partial_{od} + \overline{s_\phi(\check{M})}\right)$ and some other parts coming from the critical points. Let us look at the part coming from a_i, where the closures $\mathcal{L}_+(a_i)$ and $\mathcal{L}_-(a_i)$ of flow lines stop and closures of flow lines of $\mathcal{A}_i$ start. Consider a tubular neighborhood

$$D^2\times\mathcal{L}_+(a_i) = \{(u\exp(i\theta), y); u\in[0,1], \theta\in[0,2\pi[, y\in\mathcal{L}_+(a_i)\}$$

around $\mathcal{L}_+(a_i)$, where $\phi_t((u\exp(i\theta),y))$ reads $(u'\exp(i\theta),y')$ for some $u'\geq u$, for $t\geq 0$ and for u small enough, so that θ is preserved by the flow. When u approaches 0, the flow line through $(u\exp(i\theta),y)$ approaches $\mathcal{L}_+(a_i)\cup\mathcal{L}_\theta(\mathcal{A}_i)$ where $\mathcal{L}_\theta(\mathcal{A}_i)$ is the closure of a flow line in $\mathcal{A}_i$ determined by θ, for *generic* θ (which are θ such that

this closure does not end at a b_j). In particular, P_ϕ contains $\pm(\mathcal{L}_+(a_i)\times\mathcal{A}_i)$, and we examine more closely what P_ϕ looks like near $\big(\mathcal{L}_+(a_i)\times f^{-1}([1,+\infty[)\big)$.

Blow up 0 in D^2 to obtain an annulus $B\ell(D^2,0)$. Blow up $\mathcal{L}_+(a_i)$ in $D^2\times\mathcal{L}_+(a_i)$ to replace $\mathcal{L}_+(a_i)$ by its unit normal bundle $S^1\times\mathcal{L}_+(a_i)=\{(\exp(i\theta),y)\}$. Let $B\ell(D^2,0)\times\mathcal{L}_+(a_i)$ denote the blown-up tubular neighborhood. Fix a fiber $B\ell(D^2,0)_0=\{(u,\exp(i\theta));u\in[0,1],\exp(i\theta)\in S^1\}$ of $B\ell(D^2,0)\times\mathcal{L}_+(a_i)$, and its natural projection onto the disk $D^2_0=\{u\exp(i\theta)\}$. Then there are topological embeddings

$$\begin{array}{rccl} E_1\colon & D^2_0\times]-\infty,1[& \to & f^{-1}(]-\infty,1[) \\ & (u\exp(i\theta),x) & \mapsto & m=E_1(u\exp(i\theta),x)\end{array}$$

such that m is on the flow line through the point $u\exp(i\theta)$ of D^2_0 and $f(m)=x$, and

$$\begin{array}{rccl} E_2\colon & B\ell(D^2,0)_0\times]1,5[& \to & f^{-1}(]1,5[) \\ & (u,\exp(i\theta),x) & \mapsto & n=E_2(u,\exp(i\theta),x)\end{array}$$

such that $f(n)=x$, n is on the flow line through the point $u\exp(i\theta)$ of $B\ell(D^2,0)_0$ if $u\neq 0$, and $E_2(0,\exp(i\theta),x)\in\mathcal{L}_\theta(\mathcal{A}_i)$. Then P_ϕ intersects $f^{-1}(]-\infty,1[)\times f^{-1}(]1,5[)$ near $\mathcal{L}_+(a_i)\times f^{-1}(]1,5[)$ as the image of the continuous embedding

$$\begin{array}{rccl} E\colon & B\ell(D^2,0)_0\times]-\infty,1[\times]1,5[& \to & \check{M}^2 \\ & (u,\exp(i\theta),x_1,x_2) & \mapsto & (E_1(u\exp(i\theta),x_1),E_2(u,\exp(i\theta),x_2))\end{array}$$

and the boundary of P_ϕ contains $E(\partial_b B\ell(D^2,0)_0\times]-\infty,1[\times]1,5[)$ where

$$\partial_b B\ell(D^2,0)_0=-S^1$$

is the preimage of $(0\in D^2_0)$. The closure of $]-\infty,1[$ is naturally identified with $\mathcal{L}_+(a_i)$ via E_1, so that the boundary of P_ϕ contains $\mathcal{L}_+(a_i)\times E_2(S^1\times]1,5[)$ and it is easy to conclude that the boundary part coming from a_i near $\mathcal{L}_+(a_i)\times f^{-1}([1,+\infty[)$ is $(-\mathcal{L}_+(a_i))\times\mathcal{A}_i$ (with a minor 2–dimensional abuse of notation around a_i). We similarly find $\mathcal{L}_-(a_i)\times\mathcal{A}_i$ in ∂P_ϕ, and the part of ∂P_ϕ coming from a_i is $(\mathcal{L}_-(a_i)-\mathcal{L}_+(a_i))\times\mathcal{A}_i$.

For $\mathcal{L}_+(b_j)$, we similarly get a part of ∂P_ϕ

$$-\bigcup_{\exp(i\theta)\in S^1}\text{flow line }\mathcal{L}_\theta(\mathcal{B}_j)\times\mathcal{L}_+(b_j),$$

locally oriented as (flow line $\mathcal{L}_\theta(\mathcal{B}_j)$)$\times(S^1\times\mathcal{L}_+(b_j))$ where $\mathcal{B}_j$ locally reads $(-\mathcal{L}_\theta(\mathcal{B}_j)\times S^1)$, and the boundary part coming from b_j is $\mathcal{B}_j\times(\mathcal{L}_-(b_j)-\mathcal{L}_+(b_j))$. The two boundary parts $(-\mathcal{L}(a_i))\times\mathcal{A}_i$ and $\mathcal{B}_j\times(-\mathcal{L}(b_j))$ intersect along a two-dimensional locus, and the 3-cycle ∂P_ϕ is completely described in the statement. $\diamond$

Lemma 4.4

$$\partial P_{\mathcal{I}} = \sum_{i=1}^{g} \mathcal{L}(a_i) \times \mathcal{A}_i + \sum_{j=1}^{g} \mathcal{B}_j \times \mathcal{L}(b_j) + \sum_{c \in \mathcal{C}} \mathcal{J}_{j(c)i(c)} \sigma(c) (S^2 \times \gamma(c))$$

PROOF: The interior of a figure similar to Figure 9 embeds in the closure $\mathcal{A}_i$ of the ascending manifold of a_i in $\check{M}$. The whole closure is obtained by attaching such an open disk to the ascending manifolds ($\mathcal{L}(b_j) = \mathcal{L}_+(b_j) - \mathcal{L}_-(b_j)$) of the b_j.

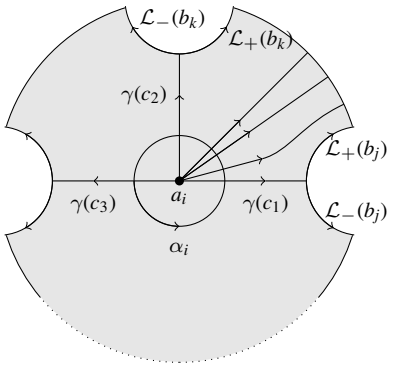

Figure 9: The interior of $\mathcal{A}_i$ (In the figure $\sigma(c_1) = 1 = -\sigma(c_2)$.)

Recall that when the sign $\sigma(c)$ of a crossing $c \in \alpha_i \cap \beta_j$ is 1, β_j is positively normal to $\mathcal{A}_i$ and α_i is positively normal to $\mathcal{B}_j$ along the interior of $\gamma(c)$. See Lemma 4.1.

When $\mathcal{A}_i$ arrives at b_j by a line $\gamma(c)$, it opens to $\mathcal{L}(b_j)$ and we find

$$\partial \mathcal{A}_i = \sum_{j=1}^{g} \sum_{c \in \alpha_i \cap \beta_j} \sigma(c) \mathcal{L}(b_j) = \sum_{j=1}^{g} \langle \alpha_i, \beta_j \rangle_{H_{a,2}} \mathcal{L}(b_j)$$

$$\partial \mathcal{B}_j = \sum_{i=1}^{g} \langle \alpha_i, \beta_j \rangle_{H_{a,2}} \mathcal{L}(a_i).$$

Near a connecting flow line $\gamma(c)$, $\mathcal{B}_j$ is parametrized by $\beta_j \times \gamma(c)(]1,5[)$ and $\mathcal{A}_i$ is parametrized by $\gamma(c)(]1,5[) \times \alpha_i$. Near the diagonal of such a line, $\mathcal{B}_j \times \mathcal{A}_i$ is parametrized by the height of the first point in $[1,5]$ followed by the tiny difference (second point minus first point) that is parametrized by (height difference, α_i, $-(-\beta_j)$), where one minus sign in front of β_j comes from the permutation of the parameters, and the other one comes from the fact that β_j is now used to parametrize the difference, so that we get $\sum_{c \in \mathcal{C}} \mathcal{J}_{j(c)i(c)} \sigma(c) (S^2 \times \gamma(c))$ in the boundary. ◇

4.3 Using the propagator to prove Proposition 3.4

Let ι denote the continuous involution of $C_2(M)$ that exchanges two points in a pair of $(\check{M}^2 \setminus \mathrm{diag})$. Note that ι reverses the orientation of $C_2(M)$.

Lemma 4.5 *For any 2–cycle $G = \sum_{(c,d)\in\mathcal{C}^2} g_{cd}(\gamma(c) \times \gamma(d)_{\|})$ of $C_2(M)$,*

$$[G] = \left[\sum_{(c,d)\in\mathcal{C}^2} g_{cd}(\gamma(d) \times \gamma(c)_{\|}) \right].$$

PROOF: With the notation of Subsection 3.2, for $\varepsilon = \pm$ and $\eta = \pm$, let

$$\gamma(c)_{\nu^\varepsilon(\mathcal{A})\nu^\eta(\mathcal{B})} = \gamma^\varepsilon_{\mathcal{A}}(c) + [c^\varepsilon_{\mathcal{A}}, c^\eta_{\mathcal{B}}] + \gamma^\eta_{\mathcal{B}}(c)$$

so that

$$\gamma(c)_{\|} = \frac{1}{4}\left(\gamma(c)_{\nu^+(\mathcal{A})\nu^+(\mathcal{B})} + \gamma(c)_{\nu^+(\mathcal{A})\nu^-(\mathcal{B})} + \gamma(c)_{\nu^-(\mathcal{A})\nu^+(\mathcal{B})} + \gamma(c)_{\nu^-(\mathcal{A})\nu^-(\mathcal{B})}\right).$$

Then for any ε and for any η,

$$G^{\varepsilon,\eta} = \sum_{(c,d)\in\mathcal{C}^2} g_{cd}\gamma(c) \times \gamma(d)_{\nu^\varepsilon(\mathcal{A})\nu^\eta(\mathcal{B})}$$

is a 2–cycle homotopic to

$$G^{\varepsilon,\eta}_s = \sum_{(c,d)\in\mathcal{C}^2} g_{cd}\gamma(c)_{\nu^{-\varepsilon}(\mathcal{A})\nu^{-\eta}(\mathcal{B})} \times \gamma(d).$$

Now,

$$\iota(G^{\varepsilon,\eta}_s) = -\sum_{(c,d)\in\mathcal{C}^2} g_{cd}\gamma(d) \times \gamma(c)_{\nu^{-\varepsilon}(\mathcal{A})\nu^{-\eta}(\mathcal{B})},$$

and, since $[\iota_*(S)] = -[S]$, ι_* is the multiplication by (-1) in $H_2(C_2(M);\mathbb{Q})$, and $(-\iota(G^{\varepsilon,\eta}_s))$ is homologous to $G^{\varepsilon,\eta}$. Since G is the average of the $G^{\varepsilon,\eta}$, and since $\left(\sum_{(c,d)\in\mathcal{C}^2} g_{cd}\gamma(d) \times \gamma(c)_{\|}\right)$ is the average of the $(-\iota(G^{\varepsilon,\eta}_s))$, the lemma is proved. $\diamond$

In order to prove Proposition 3.4, we are now left with the proof that

$$[G] = \sum_{(c,d)\in\mathcal{C}^2} g_{cd}\ell(c,d)[S].$$

We prove this by transforming the $\gamma(c)$ into

$$\gamma(c)_{\nu(\mathcal{B})} = \frac{1}{2}\left(\gamma(c)_{\nu^+(\mathcal{B})} + \gamma(c)_{\nu^-(\mathcal{B})}\right)$$

where $\gamma(c)_{\nu^+(\mathcal{B})}$ (resp. $\gamma(c)_{\nu^-(\mathcal{B})}$) is obtained from $\gamma(c)$ by pushing it much less than the distance between $\gamma(c)_{\nu^\varepsilon(\mathcal{A})\nu^\eta(\mathcal{B})}$ and $\gamma(c)$, in the direction of the positive (resp. negative) normal to $\mathcal{B}_{j(c)}$, except in the neighborhood of $a_{i(c)}$, where

- $\gamma(c)_{\nu(\mathcal{B})}$ is in $\mathcal{A}_{i(c)}$ and it is transverse to the $\mathcal{B}_j$,
- the starting points near a_i of all the $\gamma(c)_{\nu^+(\mathcal{B})}$ and the $\gamma(c)_{\nu^-(\mathcal{B})}$ for which $i(c)=i$ coincide, they are denoted by $a_{i,\nu(\mathcal{B})}$,
- this starting point $a_{i,\nu(\mathcal{B})}$ does not belong to the sheets of the $\mathcal{B}_j$ corresponding to crossings of α_i and the β_j, (these sheets meet along $\mathcal{L}(a_i)$),
- the first encountered sheet from $a_{i,\nu(\mathcal{B})}$ when turning around $\mathcal{L}(a_i)$ like α_i is the sheet of $p(\alpha_i)$.

See the local infinitesimal picture of Figure 10. Recall from Lemma 4.1 that α_i is the positive normal to $\mathcal{B}_j$ along flow lines through positive crossings.

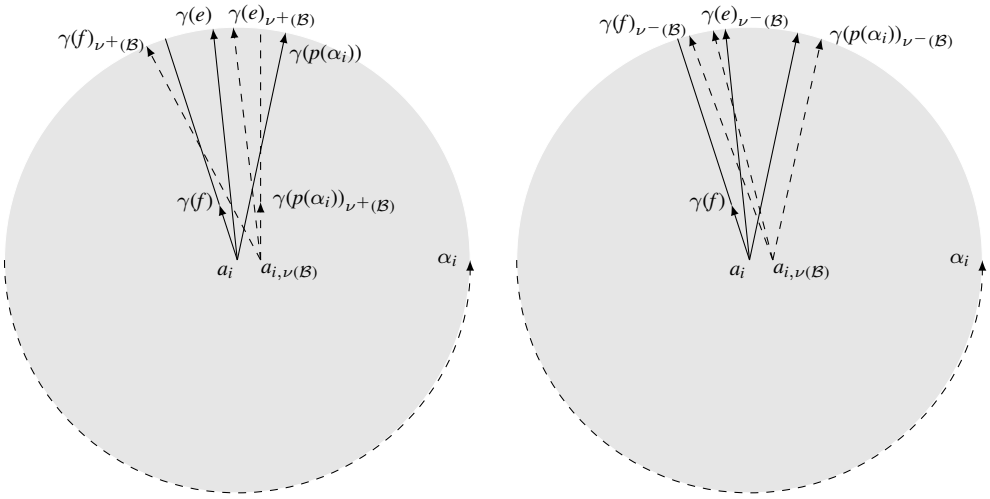

Figure 10: The $\gamma(c)_{\nu^+(\mathcal{B})}$ and the $\gamma(c)_{\nu^-(\mathcal{B})}$ near a_i (where $\sigma(p(\alpha_i))=\sigma(f)=1=-\sigma(e)$)

We shall similarly fix the positions of the

$$\gamma(d)_{\parallel}=\frac{1}{4}\left(\gamma(d)_{\nu^+(\mathcal{A})\nu^+(\mathcal{B})}+\gamma(d)_{\nu^+(\mathcal{A})\nu^-(\mathcal{B})}+\gamma(d)_{\nu^-(\mathcal{A})\nu^+(\mathcal{B})}+\gamma(d)_{\nu^-(\mathcal{A})\nu^-(\mathcal{B})}\right)$$

by homotopies of the $\gamma(d)_{\nu^\varepsilon(\mathcal{A})\nu^\eta(\mathcal{B})}=\gamma^\varepsilon_{\mathcal{A}}(d)+[d^\varepsilon_{\mathcal{A}},d^\eta_{\mathcal{B}}]+\gamma^\eta_{\mathcal{B}}(d)$, with the notation of Subsection 3.2, so that:

- for any d, $\partial\gamma(d)_{\nu^\varepsilon(\mathcal{A})\nu^\eta(\mathcal{B})}=b^\eta_{j(d)}-a^\varepsilon_{i(d)}$ is fixed,
- $\gamma(d)_{\nu^\varepsilon(\mathcal{A})\nu^\eta(\mathcal{B})}$ is on the ε side of $\mathcal{A}_{i(d)}$ except near $b_{j(d)}$ where its orthogonal projection $\gamma(d)_{\nu^\varepsilon(\mathcal{A})}$ on $\mathcal{B}_{j(d)}$ is shown in Figure 11,
- $\gamma(d)_{\nu^\varepsilon(\mathcal{A})\nu^\eta(\mathcal{B})}$ is on the η side of $\mathcal{B}_{j(d)}$ except near $a_{i(d)}$ where its orthogonal projection on $\mathcal{A}_{i(d)}$ behaves like the projection of $\gamma(d)_{\nu^\eta(\mathcal{B})}$ in Figure 10 at a larger scale.

In particular, the orthogonal projections on $\mathcal{B}_{j(d)}$ of $b^+_{j(d)}$ and $b^-_{j(d)}$ both coincide with the intersection point of the dashed segments in Figure 11, and the orthogonal projections on $\mathcal{A}_{i(d)}$ of $a^+_{i(d)}$ and $a^-_{i(d)}$ both coincide with the intersection point of the dashed segments in Figure 10 at a larger scale.

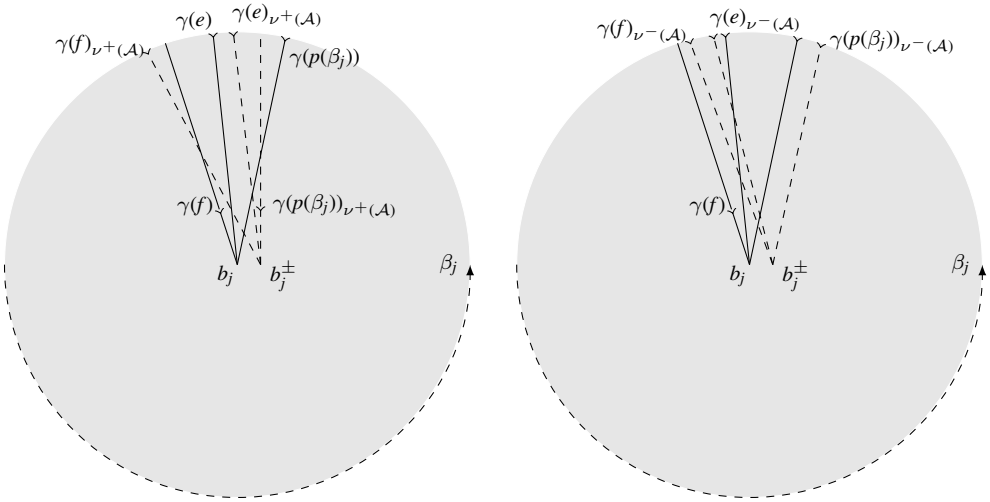

Figure 11: The orthogonal projections of the $\gamma(d)_{\|}$ on $\mathcal{B}_j$ near b_j (where $\sigma(p(\beta_j)) = \sigma(f) = 1 = -\sigma(e)$)

These positions being fixed, we have the following proposition that implies Proposition 3.4.

Proposition 4.6

$$\langle \gamma(c)_{\nu(\mathcal{B})} \times \gamma(d)_{\|}, \mathcal{P}(f,\mathfrak{g})\rangle = \ell(c,d).$$

Recall $\mathcal{P}(f,\mathfrak{g}) = P_\phi + P_{\mathcal{I}}$. We prove the proposition by computing the intersections with $P_{\mathcal{I}}$ and P_ϕ in Lemmas 4.7 and 4.8 below.

Lemma 4.7

$$\langle \gamma(c)_{\nu(\mathcal{B})} \times \gamma(d)_{\|}, \mathcal{B}_j \times \mathcal{A}_i\rangle = -\langle [p(\alpha(c)), c|_\alpha, \beta_j\rangle \langle \alpha_i, [p(\beta(d)), d|_\beta\rangle$$

PROOF: In any case, $\langle \gamma(c)_{\nu(\mathcal{B})} \times \gamma(d)_{\|}, \mathcal{B}_j \times \mathcal{A}_i\rangle_{C_2(M)} = \langle \gamma(c)_{\nu(\mathcal{B})}, \mathcal{B}_j\rangle_M \langle \gamma(d)_{\|}, \mathcal{A}_i\rangle_M$.

The only intersection points of $\gamma(c)_{\nu(\mathcal{B})}$ with $\mathcal{B}_j$ are shown in Figure 10. Then since the $\gamma(c)_{\nu(\mathcal{B})}$ cross the $\mathcal{B}_j$ like the α_i, which are positive normals for $\mathcal{B}_j$ along flow lines associated to positive crossings

$$\langle \gamma(c)_{\nu(\mathcal{B})}, \mathcal{B}_j\rangle_M = \langle [p(\alpha(c)), c|_{\alpha(c)}, \beta_j\rangle.$$

The computation of $\langle \gamma(d)_{\|}, \mathcal{A}_i \rangle_M$ is similar since the position of the $\gamma(d)_{\|}$ with respect to $\mathcal{B}_j$ does not matter. The only difference comes from the fact that the flow lines are oriented towards $b_{j(d)}$ so that they cross the $\mathcal{A}_i$ like $(-\beta_j)$, which is the positive normal along flow lines associated to negative crossings. See Figure 11.

$$\langle \gamma(d)_{\|}, \mathcal{A}_i \rangle_M = -\langle \alpha_i, [p(\beta(d)), d|_{\beta(d)} \rangle.$$

$\diamond$

Lemma 4.8

$$\langle \gamma(c)_{\nu(\mathcal{B})} \times \gamma(d)_{\|}, P_\phi \rangle = \langle [p(\alpha(c)), c|_\alpha, [p(\beta(d)), d|_\beta \rangle.$$

PROOF: Assume $c \in \alpha_i \cap \beta_{j(c)}$ and $d \in \alpha_{i(d)} \cap \beta_j$. When the first $\check{M}$-coordinate of a point of P_ϕ is in $\gamma(c) \setminus a_i$, its second $\check{M}$-coordinate is in $\big(\gamma(c) \cup \mathcal{L}(b_{j(c)})\big)$, and therefore it is not in $\gamma(d)_{\|}$. Since the first $\check{M}$-coordinate of a point in $\gamma(c)_{\nu(\mathcal{B})} \times \gamma(d)_{\|}$ is very close to $\gamma(c)$, $\gamma(c)_{\nu(\mathcal{B})} \times \gamma(d)_{\|}$ intersects P_ϕ in a small neighborhood of $a_i \times \mathcal{A}_i$.

Thus, the intersection points will be very close to pairs of points on flow rays from a_i on $\mathcal{A}_i$, the closest point to a_i being on $\gamma(c)_{\nu(\mathcal{B})}$ and the second one on $\gamma(d)_{\|}$. Then, for a given $\gamma(c)$, the second point must be on the subsurface $D(\gamma(c))$ of $\mathcal{A}_i$ made of the points x such that the flow ray from a_i to x intersects $\gamma(c)_{\nu^+(\mathcal{B})}$ or $\gamma(c)_{\nu^-(\mathcal{B})}$. This interaction locus of $\gamma(c)_{\nu^+(\mathcal{B})}$, $D(\gamma(c))$, is shown in Figure 12. The interaction locus of $\gamma(c)_{\nu^-(\mathcal{B})}$ is similar.

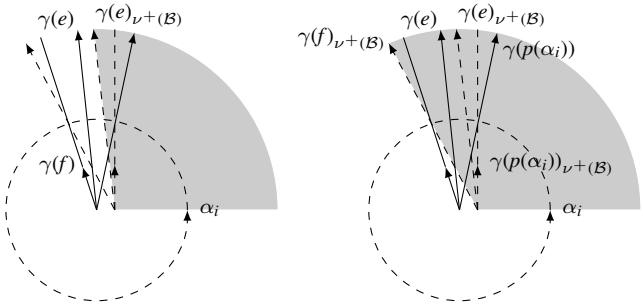

Figure 12: Interaction loci of $\gamma(e)_{\nu^+(\mathcal{B})}$ and $\gamma(f)_{\nu^+(\mathcal{B})}$ on $\mathcal{A}_i$ (where $\sigma(f) = 1 = -\sigma(e)$)

The only intersection points of $\gamma(d)_{\|}$ with the domain $D(\gamma(c))$ of $\mathcal{A}_i$ are near the b_j and they are shown in Figure 11.

The curve $\gamma(d)_{\|}$ meets $\mathcal{A}_i$ near a crossing line $\gamma(e)$, where *near* means in the sheet of $\gamma(e)$ around $\mathcal{L}(b_j)$,

- with probability 1 if $i(e) = i$ and if $e \in [p(\beta_j), d[_{\beta_j}$,
- with probability $1/2$ (depending on the side of $\mathcal{A}_i$ for $\gamma(d)_{\|}$ near b_j) if $i(e) = i$ and if $e = d$, (this is also valid when $e = p(\beta_j) = d$),
- with probability 0 in the other cases.

The corresponding intersection point is in $D(\gamma(c))$ if $e \in [p(\alpha_i), c[_{\alpha_i}$, or if $e = c$ and $\gamma(d)_{\|}$ is on the correct side of $\mathcal{B}_j$ (the $((-\alpha_i)$ side), that is with a probability $1/2$ independent of the previous one.

Then M is oriented as (flow line $\times\, \gamma(c)_{\nu(\mathcal{B})} \times \nu^+(\mathcal{A}_i)$) near a_i and P_ϕ is oriented as

$$\text{(beginning of flow line} \times \text{diag}(\gamma(c)_{\nu(\mathcal{B})} \times \nu^+(\mathcal{A}_i)) \times \text{end of flow line)},$$

which is intersected negatively by $\gamma(c)_{\nu(\mathcal{B})} \times \nu^+(\mathcal{A}_i)$, where $\nu^+(\mathcal{A}_i)$ is oriented like $\sigma(e)\beta_j$ and like $(-\sigma(e))\gamma(d)_{\|}$ near a point in $\big(\gamma(c)_{\nu(\mathcal{B})} \times \gamma(d)_{\|}\big) \cap P_\phi$ corresponding to a crossing e of $[p(\alpha(c)), c|_\alpha \cap [p(\beta(d)), d|_\beta$. $\diamond$

5 The combing associated with $\mathfrak{m}$ and its associated propagator

In this section, we first define the combing $X(w, \mathfrak{m})$ of $\check{M}$. Next we introduce correction 4-chains P_h and P_Σ in $U\check{M} \subset \partial C_2(M)$ such that the sum $\mathcal{P} = \mathcal{P}(f, \mathfrak{g}) + P_h + P_\Sigma$ is a propagator associated with $X(w, \mathfrak{m})$.

5.1 The combing $X(w, \mathfrak{m})$

Consider the matching $\mathfrak{m}$ introduced in Subsection 3.5. Up to renumbering and reorienting the $\mathcal{B}_j$, assume that $c_i \in \alpha_i \cap \beta_i$ and that $\sigma(c_i) = 1$. Set $\gamma_i = \gamma(c_i)$.

There is a combing $X = X(w, \mathfrak{m})$ (section of the unit tangent bundle) of $\check{M}$ that coincides with the direction s_ϕ of the flow (and the gradient of f) outside the union of regular neighborhoods $N(\gamma_i)$ of the γ_i, that is opposite to s_ϕ along the interiors of the γ_i and that is obtained as follows on $N(\gamma_i)$. Choose a natural trivialization (X_1, X_2, X_3) of $T\check{M}$ on a regular neighborhood $N(\gamma_i)$ of γ_i, such that:

- γ_i is directed by X_1,
- the other flow lines never have X_1 as an oriented tangent vector,

- (X_1, X_2) is tangent to $\mathcal{A}_i$ (except on the parts of $\mathcal{A}_i$ near b_i that come from other crossings of $\alpha_i \cap \beta_i$), and (X_1, X_3) is tangent to $\mathcal{B}_i$ (except on the parts of $\mathcal{B}_i$ near a_i that come from other crossings of $\alpha_i \cap \beta_i$).

This parallelization identifies the unit tangent bundle $UN(\gamma_i)$ of $N(\gamma_i)$ with $S^2 \times N(\gamma_i)$.

There is a homotopy $h\colon [0,1] \times (N(\gamma_i) \setminus \gamma_i) \to S^2$, such that

- h_0 is the unit tangent vector to the flow lines of ϕ,
- h_1 is the constant map to $(-X_1)$ and
- $h_t(y)$ goes from $h_0(y) = s_\phi(y)$ to $(-X_1)$ along the shortest geodesic arc of S^2 from $s_\phi(y)$ to $(-X_1)$, which is denoted by $[s_\phi(y), -X_1]$.

Let 2η be the distance between γ_i and $\partial N(\gamma_i)$ and let $X(y) = h(\max(0, 1-d(y,\gamma_i)/\eta), y)$ on $N(\gamma_i) \setminus \gamma_i$, and $X = -X_1$ along γ_i.

Note that X is tangent to $\mathcal{A}_i$ on $N(\gamma_i)$ (except on the parts of $\mathcal{A}_i$ near b_i that come from other crossings of $\alpha_i \cap \beta_i$), and that X is tangent to $\mathcal{B}_i$ on $N(\gamma_i)$ (except on the parts of $\mathcal{B}_i$ near a_i that come from other crossings of $\alpha_i \cap \beta_i$). More generally, project the normal bundle to γ_i to $\mathbb{R}^2$ in the X_1–direction by sending γ_i to 0, $\mathcal{A}_i$ to an axis $\mathcal{L}_i(\mathcal{A})$ and $\mathcal{B}_i$ to an axis $\mathcal{L}_i(\mathcal{B})$. Then the projection of X goes towards 0 along $\mathcal{L}_i(\mathcal{B})$ and starts from 0 along $\mathcal{L}_i(\mathcal{A})$, it has the direction of $\sigma_a(y)$ at a point y of $\mathbb{R}^2$ near 0, where σ_a is the planar reflexion that fixes $\mathcal{L}_i(\mathcal{A})$ and reverses $\mathcal{L}_i(\mathcal{B})$. See Figure 13.

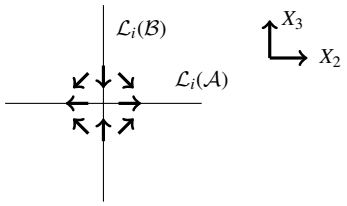

Figure 13: Projection of X

Then $X(y)$ is on the half great circle that contains $\sigma_a(y)$, X_1 and $(-X_1)$. In Figure 14 (and in Figure 7), γ_i is a vertical segment, all the other flow lines corresponding to crossings involving α_i go upwards from a_i, and X is simply the upward vertical field. See also Figure 20.

5.2 The propagator associated with a combed Heegaard splitting

Recall that $UN(\gamma_i)$ is identified with $S^2 \times N(\gamma_i)$. Let $P_h = P_h(\mathfrak{m})$ be the closure in $\partial C_2(M)$ of the image of $\{(t,y); t \in [0, \max(0, 1 - d(y,\gamma_i)/\eta)], y \in N(\gamma_i) \setminus \gamma_i\}$ in

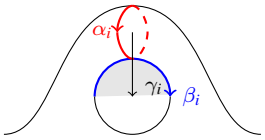

Figure 14: γ_i

$S^2 \times (N(\gamma_i))$ under $((t,y) \mapsto (h(t,y),y))$.

Lemma 5.1 $\partial P_h = \overline{X(\check{M})} - \overline{s_\phi(\check{M})} - \sum_{i=1}^g U\check{M}_{|\gamma_i}$

PROOF: We explain the $(U\check{M}_{|\gamma_i} = S^2 \times \gamma_i)$ part of ∂P_h, with its sign. The homotopy h naturally extends to $[0,1] \times B\ell(N(\gamma_i),\gamma_i)$, where $B\ell(N(\gamma_i),\gamma_i)$ is obtained from $N(\gamma_i)$ by blowing up γ_i, so that $(-B\ell(N(\gamma_i),\gamma_i))$ contains the unit normal bundle $S^1 \times \gamma_i$ of γ_i in C_M, in its boundary. Then ∂P_h contains $\{(h(t,y), p_{\gamma_i}(y)) \in S^2 \times \gamma_i; t \in [0,1], y \in S^1 \times \gamma_i\}$, where S^1, which is the blown-up center of the fiber D^2 of $N(\gamma_i)$, is mapped by σ_a to the equator of S^2 so that the image of $([0,1] \times S^1)$ covers a fiber S^2 of $U\check{M}_{|\gamma_i}$ with degree (-1). ◇

Recall the 1–cycle $L(\mathfrak{m}) = \sum_{i=1}^g \gamma_i - \sum_{c\in\mathcal{C}} \mathcal{J}_{j(c)i(c)}\sigma(c)\gamma(c)$. Let $\Sigma(\mathfrak{m})$ be a two–chain bounded by $L(\mathfrak{m})$ in $\check{M}$ and let

$$P_\Sigma = U\check{M}_{|\Sigma(\mathfrak{m})}.$$

Note that P_Σ is homeomorphic to $S^2 \times \Sigma(\mathfrak{m})$.

Proposition 5.2

$$\mathcal{P} = \mathcal{P}(f,\mathfrak{g}) + P_h + P_\Sigma$$

is a propagator associated with the combing $X(w,\mathfrak{m})$.

PROOF: The boundary of $\mathcal{P}$ is $(\overline{X(w,\mathfrak{m})(\check{M})} + \partial_{od})$. ◇

Recall that ι denotes the involution of $C_2(M)$ that exchanges two points in a pair. Then $\iota(\mathcal{P})$ is also a propagator associated with the combing $(-X(w,\mathfrak{m}))$. Theorem 2.1 defines $\Theta(M, X(w,\mathfrak{m}))$ from the algebraic intersection of $\mathcal{P}$ and $\iota(\mathcal{P})$, which we compute from now on in order to prove Theorem 3.8.

6 Computation of $[\mathcal{P}_{X(w,\mathfrak{m})} \cap \mathcal{P}_{-X(w,\mathfrak{m})}]$

6.1 A description of $[\mathcal{P}_{X(w,\mathfrak{m})} \cap \mathcal{P}_{-X(w,\mathfrak{m})}]$

Fix w, $\mathfrak{m}$, $X = X(w,\mathfrak{m})$, $L = L(\mathfrak{m})$ and $\Sigma = \Sigma(\mathfrak{m})$ such that $\partial\Sigma = L$.

Consider a vector field Y of $X^\perp$ on $\check{M}$ such that

- Y vanishes outside C_M,
- the norm of Y is one on the $\gamma(c)$,
- for every i, $Y(a_i)$ is tangent to the line $\mathcal{L}(a_i)$, which is the descending manifold of a_i, (but $Y(a_i)$ does not necessarily direct the line),
- for every j, $Y(b_j)$ is tangent to the line $\mathcal{L}(b_j)$, (again, $Y(b_j)$ does not necessarily direct the line),

Then $L_{\|Y}$ denotes the link parallel to L obtained by pushing L in the Y direction. Along $\gamma(c)$, σ_a is the symmetry of $X^\perp$ with respect to $\mathcal{A}_{i(c)}$ that preserves the vectors tangent to $\mathcal{A}_{i(c)}$ and reverses the vectors tangent to $\mathcal{B}_{j(c)}$. Define $\gamma(c) \times \gamma(d)_{\|\sigma_a(-Y)}$ as the product of $\gamma(c)$ and a parallel of $\gamma(d)$ "infinitely" close to $\gamma(d)$ in the direction of $\sigma_a(-Y)$. This can be formalised as follows. When $c \neq d$, $\gamma(c) \times \gamma(d)_{\|\sigma_a(-Y)} = \gamma(c) \times \gamma(d)$ (away from the possibly coinciding ends). For $x \in \gamma(c)$, let $\gamma'_x(c)$ denote the unit tangent vector of $\gamma(c)$ at x that orients $\gamma(c)$, and let $[-\gamma'_x(c), \gamma'_x(c)]_{\sigma_a(-Y)}$ denote the half great circle in the fiber $U\check{M}_{|x}$ through $\sigma_a(-Y(x))$ towards $\gamma'_x(c)$. Let $s_{[-\gamma'(c),\gamma'(c)]_{\sigma_a(-Y)}}(\gamma(c))$ be the total space of the bundle over $\gamma(c)$ of these half-circles. Then

$$\gamma(c) \times \gamma(c)_{\|\sigma_a(-Y)} = \overline{\gamma(c)^2 \setminus \mathrm{diag}(\gamma(c)^2)} - s_{[-\gamma'(c),\gamma'(c)]_{\sigma_a(-Y)}}(\gamma(c)).$$

Similarly, $s_{[-X,X]_{\sigma_a(-Y)}}(\partial\Sigma)$ is the total space of the bundle over $\partial\Sigma$ of the half-circles $[-X,X]_{\sigma_a(-Y)}$. In this section, we prove the following proposition.

Proposition 6.1 *Let Y be a vector field of $X^\perp$ as above. There exists a two-chain $O(\sigma_a(-Y))$ in the hemispheres centered at $\sigma_a(-Y)$ in $U\check{M}_{|\cup_i a_i \cup (\cup_j b_j)}$ such that*

$$\begin{aligned} G^i_{\uparrow\downarrow}(Y) = \quad & \textstyle\sum_{(i,j,k,\ell)\in\{1,\dots,g\}^4} \mathcal{J}_{ji}\mathcal{J}_{\ell k} \left((\mathcal{B}_j \cap \mathcal{A}_k) \times (\mathcal{B}_\ell \cap \mathcal{A}_i)_{\|\sigma_a(-Y)}\right) \\ & - \textstyle\sum_{c\in\mathcal{C}} \mathcal{J}_{j(c)i(c)}\sigma(c) \left(\gamma(c) \times \gamma(c)_{\|\sigma_a(-Y)}\right) \\ & + O(\sigma_a(-Y)) \end{aligned}$$

is a 2–cycle of $C_2(M)$ whose homology class is unambiguously defined. Let S be a fiber of $U\check{M}$ and let $X(\Sigma)$ denote the graph of $X_{|\Sigma}$ in $U\check{M}$. Set

$$G^b_{\uparrow\downarrow}(X,Y) = lk(L, L_{\|Y})S - \left(X(\Sigma) - (-X)(\Sigma) - s_{[-X,X]_{\sigma_a(-Y)}}(\partial\Sigma)\right).$$

Then the cycle

$$G_{\uparrow\downarrow} = G^i_{\uparrow\downarrow}(Y) + G^b_{\uparrow\downarrow}(X,Y)$$

represents the homology class of $\mathcal{P}_{X(w,\mathfrak{m})} \cap \mathcal{P}_{-X(w,\mathfrak{m})}$.

6.2 Introduction to specific chains $\mathcal{P}_X$ and $\mathcal{P}_{-X}$

In this subsection, we deform the propagators $\mathcal{P}$ and $\iota(\mathcal{P})$ constructed in Section 5.2 to propagators $\mathcal{P}_X$ and $\mathcal{P}_{-X}$ that are transverse to each other, in order to determine their algebraic intersection.

Let $[-1,0]\times\partial C_2(M)$ be a (topological) collar of $\partial C_2(M)$ in $C_2(M)$. Then $C_2(M)$ is homeomorphic to $\tilde{C}_2(M) = C_2(M)\setminus(]-1/2,0]\times\partial C_2(M))$ by the *shrinking homeomorphism*

$$\begin{array}{rlcl} h_s\colon & C_2(M) & \to & \tilde{C}_2(M) \\ & (t,x)\in[-1,0]\times\partial C_2(M) & \mapsto & ((t-1)/2,x)\in[-1,-1/2]\times\partial C_2(M) \end{array}$$

that is the identity map outside the collar. Identifying $[-1/2,0]$ with $[0,6]$ by the appropriate affine monotonous transformation identifies $C_2(M)$ with

$$\tilde{C}_2(M)\cup_{\partial\tilde{C}_2(M)}([0,6]\times\partial C_2(M))\,,$$

which is our space $C_2(M)$ from now on.

Use h_s to shrink $\mathcal{P}(f,\mathfrak{g})$ and $\iota(\mathcal{P}(f,\mathfrak{g}))$ into $\tilde{C}_2(M)$, and construct transverse $\mathcal{P}_X$ and $\mathcal{P}_{-X}$ with respective boundaries $\{6\}\times\partial\mathcal{P}_X$ and $\{6\}\times\partial\mathcal{P}_{-X}$ as follows:

$$\begin{aligned} \mathcal{P}_{-X} = \;& h_s(\iota(\mathcal{P}(f,\mathfrak{g}))) + [0,1]\times\partial\iota(\mathcal{P}(f,\mathfrak{g})) \\ & +\{1\}\times\iota(P_h) + [1,3]\times(\iota(-S^2\times L+\partial_{od}) + \overline{(-X)(\check{M})}) \\ & +\{3\}\times\iota(S^2\times\Sigma) + [3,6]\times(\overline{(-X)(\check{M})} + \iota(\partial_{od})) \end{aligned}$$

while the following expression of $\mathcal{P}_X$, which is partially schematically drawn in Figure 15, will require a perturbating diffeomorphism Ψ of $C_2(M)$ isotopic and very close to the identity map in order to get transversality near the diagonal.

$$\begin{aligned} \mathcal{P}_X = \;& h_s(\Psi(\mathcal{P}(f,\mathfrak{g}))) + [0,2]\times\partial\Psi(\mathcal{P}(f,\mathfrak{g})) \\ & +\{2\}\times\Psi(P_h) + [2,4]\times\Psi(-S^2\times L+\overline{X(\check{M})}+\partial_{od}) \\ & +\{4\}\times\Psi(S^2\times\Sigma) + [4,5]\times\Psi(\overline{X(\check{M})}+\partial_{od}) \\ & +\{5\}\times\Psi_{[\varepsilon,0]}(\partial\mathcal{P}_X) + [5,6]\times\partial\mathcal{P}_X \end{aligned}$$

where $\Psi_{[\varepsilon,0]}(\partial\mathcal{P}_X)$ is the small cobordism between $\Psi(\overline{X(\check{M})}+\partial_{od})$ and $\partial\mathcal{P}_X$ induced by the isotopy between Ψ and the identity map. We describe Ψ in the next subsection.

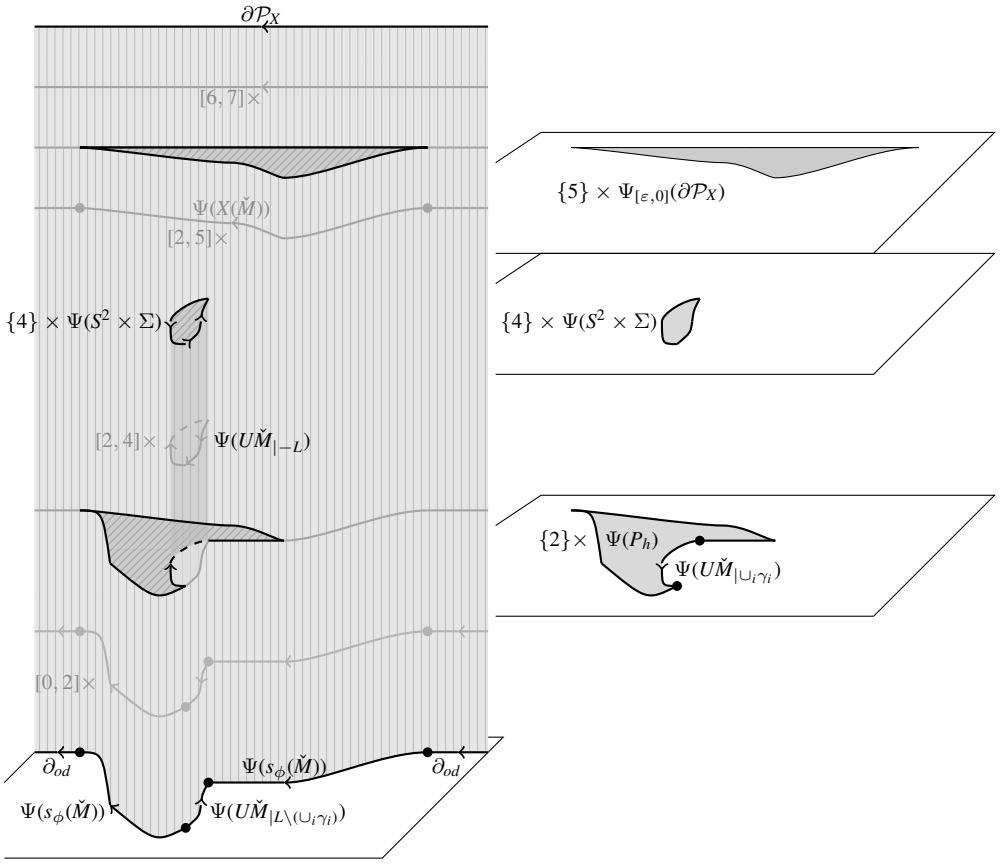

Figure 15: $\mathcal{P}_X\cap([0,6]\times\partial C_2(M))$ and its horizontal pieces

6.3 The perturbating diffeomorphism $\Psi_{Y,\varepsilon}$ of $C_2(M)$

Recall that Y is a field like in Section 6.1. For η small enough, we have an isotopy $\psi_Y\colon[0,\eta]\times\check{M}\to\check{M}$ such that $\frac{d}{dt}\psi_Y(t,y)=Y(y)$ and ψ_0 is the identity.

Let

$$\begin{array}{rccc}\chi_\varepsilon\colon & [0,\varepsilon] & \to & [0,\varepsilon]\\ & 0 & \mapsto & \varepsilon\\ & \varepsilon & \mapsto & 0\end{array}$$

be a smooth family of decreasing functions with horizontal tangents at 0 and ε for $\varepsilon\in[0,\eta]$.

Fix ε. Consider the diffeomorphism $\Psi = \Psi_{Y,\varepsilon}$ of $C_2(\check{M})$ that is the identity outside a neighborhood $U\check{M} \times [0,\varepsilon]$ of the blown-up diagonal, where the second coordinate stands for the distance between two points in a pair, and that reads

$$(v \in U\check{M}_{|m}, u) \mapsto (T\psi_Y(\chi_\varepsilon(u), m)(0, v), u)$$

on $U\check{M} \times [0,\varepsilon]$, so that it coincides with $T\psi$ on $(U\check{M} = U\check{M} \times \{0\})$, where $\psi = \psi_Y(\varepsilon, .)$.

Define the flow $\psi\phi\psi^{-1}$ $((t,m) \mapsto \psi\phi_t\psi^{-1}(m))$ on $\check{M}$. Observe

$$\Psi(\overline{s_\phi(\check{M})}) = s_{\psi\phi\psi^{-1}}(\check{M}).$$

The projections of the directions of the flow lines of $\psi_*(\phi) = \psi\phi\psi^{-1}$ onto a fiber of the tubular neighborhood of a line $\gamma(c)$ are shown in Figure 16. We shall refer to the directions of these projections as *horizontal* directions.

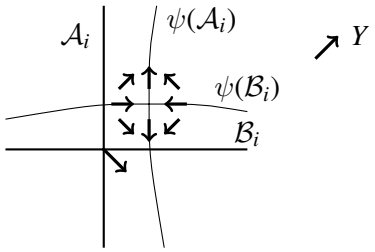

Figure 16: Horizontal directions of the flow lines of $\psi_*(\phi)$

Without loss, assume that the isotopy ψ_Y moves the critical points a_i along the lines $\mathcal{L}(a_i)$ and the b_j along the $\mathcal{L}(b_j)$ (recall that Y is tangent to these lines). Let $\overline{\phi}$ denote the flow ϕ reversed so that $\iota(P_\phi) = P_{\overline{\phi}}$.

Lemma 6.2 *For ε small enough, the direction of $\psi_*(\phi)$ (which is the direction of $s_{\psi_*(\phi)}$) along $\gamma(c)$ is very close to a geodesic arc between the direction of ϕ and $\sigma_a(-Y)$, so that its distance in S^2 from $\sigma_a(Y)$ is at least $\pi/4$.*

The direction of $\overline{\phi}$ along $\psi(\gamma(c))$ is very close to a geodesic arc between the direction of $(-T(\psi(\gamma(c))))$ and $\sigma_a(-Y)$, so that its distance in S^2 from $\sigma_a(Y)$ is at least $\pi/4$.

Furthermore, the direction of $\psi_*(\phi)$ at the critical points and the direction of $\overline{\phi}$ at their images under ψ coincide with $\sigma_a(-Y)$.

PROOF: Away from the ends of $\gamma(c)$, the direction of $\psi_*(\phi)$ along $\gamma(c)$ is very close to the tangent direction of $\gamma(c)$, and it is slightly deviated in the orthogonal direction

of $\sigma_a(-Y)$ since $\gamma(c)$ is obtained from $\psi(\gamma(c))$ by a translation of $-Y$. See Figure 16 and Subsection 5.1. Near the critical points, the direction of $\psi_*(\phi)$ approaches the direction of $\sigma_a(-Y)$, and it reaches it at the critical points. Similarly, the direction of $\overline{\phi}$ along $\psi(\gamma(c))$ is very close to the direction of $(-T(\gamma(c)))$ away from the ends and it is slightly deviated in the orthogonal direction of $(-\sigma_a(Y))$. Near the critical points, the direction of $\overline{\phi}$ approaches the direction of $\sigma_a(-Y)$, and it reaches it at the critical points. ◇

Lemma 6.3 $\lim_{\varepsilon\to 0}\Psi(P_\phi)\cap\iota(P_\phi)$ *is discrete located at the points* $s_{\sigma_a(-Y)}(a_i)$ *and* $s_{\sigma_a(-Y)}(b_j)$ *of* $U\check{M}$*, which are the unit tangent vectors directed by* $\sigma_a(-Y)$ *at the critical points.*

PROOF: Observe that $P_\phi\cap\iota(P_\phi)$ is supported on the restrictions of $U\check{M}$ to the critical points. Therefore, for ε small enough, $\Psi(P_\phi)\cap\iota(P_\phi)$ will be near the restrictions of $U\check{M}$ to the critical points. There are 4g points of type $s_{\overline{\phi}}(\psi(a_i))$, $s_{\psi_*(\phi)}(a_i)$, $s_{\overline{\phi}}(\psi(b_j))$ and $s_{\psi_*(\phi)}(b_j)$ in the intersection. They have the wanted direction thanks to Lemma 6.2. Except for those points we have to look for flow lines for ϕ and flow lines for $\psi_*(\phi)$ that intersect twice and that connect the intersection points with opposite directions. Under our assumptions, this can only happen on the lines $\mathcal{L}(c)$ between c and $\psi(c)$ for a critical point c. Indeed, outside $\mathcal{L}(c)$, ϕ and $\psi_*(\phi)$ both escape from the neighborhoods of $\mathcal{L}(c)$ if $c=a_i$, or both get closer if $c=b_i$. On these lines, the only parts where ϕ and $\psi_*(\phi)$ have opposite directions is between c and $\psi(c)$, and the tangent direction to $\overline{\phi}$ is the direction of $\sigma_a(-Y)$. ◇

6.4 Reduction of the proof of Proposition 6.1

Consider a regular neighborhood N of the union of the $\gamma(c)$ that contains the $\psi(\gamma(c))$, and consider the fiber bundle over N whose fibers are the complement of an open disk of radius $\pi/4$ around $\sigma_a(Y)$ in the fibers of UN. Let E be the total space of this bundle and let $\mathcal{N}=[-1,0]\times E\subset[-1,0]\times\partial C_2(M)\subset C_2(M)$. Then $H_2(\mathcal{N};\mathbb{Z})=0$.

Without loss, the chains $\mathcal{P}_X$ and $\mathcal{P}_{-X}$ are now assumed to be transverse so that their intersection I is a 2–cycle of $C_2(M)$, which we are going to compute piecewise. We shall neglect the pieces in $\mathcal{N}$ and write them as $O(\mathcal{N})$ in the statements. Sometimes, we shall also add arbitrary pieces in $\mathcal{N}$ in order to close some 2–chains and find some 2–cycle I' such that

$$I'=I+O(\mathcal{N})$$

so that I' will be homologous to I.

We shall also consider continuous limits when possible to simplify the expressions as in Lemma 6.3, which now reads:

$$\lim_{\varepsilon\to 0} \Psi(P_\phi)\cap\iota(P_\phi) = O(\mathcal{N})$$

or,
for $\varepsilon>0$ small enough, $\Psi(P_\phi)\cap\iota(P_\phi)=O(\mathcal{N})$.

For example,

$$\begin{aligned}\mathcal{P}_X\cap\mathcal{P}_{-X}\cap([5/2,6]\times\partial C_2(M)) &= [5/2,3]\times(\psi_*(X)(L)-(-X)(\psi(L)))\\ &\quad +\{3\}\times(-\psi_*(X)(\Sigma)+S^2\times(\psi(L)\cap\Sigma))\\ &\quad -[3,4]\times(-X)(\psi(L))\\ &\quad +\{4\}\times(-X)(\psi(\Sigma))\\ &= \{3\}\times(-\psi_*(X))(\Sigma)+\{4\}\times(-X)(\psi(\Sigma))\\ &\quad +\{3\}\times S^2\times(\psi(L)\cap\Sigma)+O(\mathcal{N}).\end{aligned}$$

Then $S^2\times(\psi(L)\cap\Sigma)$ is a disjoint union of spheres homologous to $lk(L,L_{\|Y})[S]$. Let

$$\ell = \lim_{\varepsilon\to 0}\left(-\{3\}\times(\psi_*(X))(\Sigma)+\{4\}\times(-X)(\psi(\Sigma))\right).$$

$$\begin{aligned}\ell &= -\{3\}\times X(\Sigma)+\{4\}\times(-X)(\Sigma)\\ &= -\{3\}\times X(\Sigma)+\{4\}\times(-X)(\Sigma)\\ &\quad -[3,4]\times(-X)(L)+\{3\}\times s_{[-X,X]_{\sigma_a(-Y)}}(L)+O(\mathcal{N})\end{aligned}$$

where the last equality comes from the fact that both $[3,4]\times(-X)(L)$ and $\{3\}\times s_{[-X,X]_{\sigma_a(-Y)}}(L)$ are in $\mathcal{N}$. Then $\mathcal{P}_X\cap\mathcal{P}_{-X}\cap([5/2,6]\times\partial C_2(M))$ is homologous to $G^b_{\uparrow\downarrow}(X,Y)$ mod $\mathcal{N}$ and the proof of Proposition 6.1 is reduced to the proof of the two following propositions.

Proposition 6.4

$$\mathcal{P}_X\cap\mathcal{P}_{-X}\cap\tilde{C}_2(M) = G^i_{\uparrow\downarrow}(Y)+O(\mathcal{N}).$$

Proposition 6.5

$$\mathcal{P}_X\cap\mathcal{P}_{-X}\cap\left([0,5/2]\times\partial C_2(M)\right) = O(\mathcal{N}).$$

In particular, $G^i_{\uparrow\downarrow}(Y)$ may be thought of as the intersection of $\mathcal{P}(f,\mathfrak{g})\cap\mathcal{P}(-f,\mathfrak{g})$ in the interior of $C_2(M)$, while $G^b_{\uparrow\downarrow}(Y)$ collects the intersection coming from the boundary corrections.

6.5 Proof of Proposition 6.4

Lemma 6.6

$$\lim_{\varepsilon\to 0}\Psi(P_{\mathcal{I}})\cap\iota(P_{\mathcal{I}})=\sum_{(i,j,k,\ell)\in\{1,\dots,g\}^4}\mathcal{J}_{ji}\mathcal{J}_{\ell k}(\mathcal{B}_j\cap\mathcal{A}_k)\times(\mathcal{B}_\ell\cap\mathcal{A}_i)_{\|\sigma_a(-Y)}+O(\mathcal{N}).$$

PROOF: The intersection $\mathcal{B}_j\times\mathcal{A}_i\cap(\mathcal{A}_k\times\mathcal{B}_\ell)$ is cooriented by the positive normals of $\mathcal{B}_j$, $\mathcal{A}_i$, $\mathcal{A}_k$ and $\mathcal{B}_\ell$ in this order. Therefore the intersection reads as in the statement of the lemma away from the diagonal. Near the diagonal and away from the critical points, $\mathcal{A}_i$ and $\mathcal{B}_j$ are moved in the direction of Y. If $Y=\vec{a}+\vec{b}$ where $\vec{a}$ is tangent to $\mathcal{A}_k$ and $\vec{b}$ is tangent to $\mathcal{B}_\ell$, then abusively write $\mathcal{A}_i=\mathcal{A}_k+\vec{b}$ and $\mathcal{B}_j=\mathcal{B}_\ell+\vec{a}$ and see that the difference of the two points is moved in the direction $(\vec{b}-\vec{a})$ of $\sigma_a(-Y)$, so that the corresponding intersection sits inside the neglected part $\mathcal{N}$. (When two points vary along the same $\gamma(c)$, the second one will be deviated in the direction of $\sigma_a(-Y)$ so that the limit pairs of points describe an arc in $U\check{M}_{|\gamma(c)}$ from $-\gamma'(c)$ to $\gamma'(c)$ through $\sigma_a(-Y)$, that is along the half great circle $[-\gamma'(c),\gamma'(c)]_{\sigma_a(-Y)}$.)

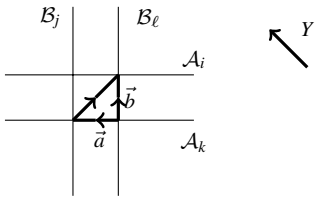

Figure 17: Deviation near the diagonal

Near a critical point, two points can come from different crossings. Then the direction between them in $(\mathcal{B}_j\cap\mathcal{A}_k)\times(\mathcal{B}_\ell\cap\mathcal{A}_i)\setminus\text{diag}$ is orthogonal to $Y=\pm\sigma_a(Y)$. The field Y can be assumed to preserve the $\mathcal{B}$-sheets near the a_i and the $\mathcal{A}$-sheets near the b_j. Then the difference of the two points is moved in the direction of $\sigma_a(-Y)$ so that it belongs to the hemisphere centered at $\sigma_a(-Y)$. ◇

Lemma 6.7

$$\lim_{\varepsilon\to 0}\Psi(P_\phi)\cap\iota(P_{\mathcal{I}})=\sum_{c\in\mathcal{C}}\mathcal{J}_{j(c)i(c)}(-\sigma(c))\overline{\{(\gamma(c)(t_1),\gamma(c)(t_2));t_1<t_2\}}+O(\mathcal{N}).$$

PROOF: The intersection $P_\phi\cap\left(\iota(P_{\mathcal{I}})=\sum_{(i,j)\in\{1,\dots,g\}^2}\mathcal{J}_{ji}\mathcal{A}_i\times\mathcal{B}_j\right)$ is supported on the

$$\overline{\{(\gamma(c)(t_1),\gamma(c)(t_2));t_1<t_2\}}$$

away from the unit bundles of the critical points. It is transverse except near these unit bundles.

Let $c \in \alpha_i \cap \beta_j$. Along $\gamma(c)$, $\mathcal{A}_i \times \mathcal{B}_j$ is cooriented by $\beta_j \times \alpha_i$. Then $P_\phi \cap (\mathcal{A}_i \times \mathcal{B}_j)$ will be oriented as $(-\sigma(c))\{(\gamma(c)(t_1), \gamma(c)(t_2)); t_1 < t_2\}$. Since $\psi_*(\phi)$ is almost vertical away from the critical points, we are left with the behaviour near the critical points. Near a_i on $\mathcal{A}_i$, (or near b_j on $\mathcal{B}_j$) the direction of $\psi_*(\phi)$ is in the hemisphere centered at $\sigma_a(-Y)$, according to Lemma 6.2, so that the pairs of points of $\mathcal{A}_i \times \mathcal{B}_j$ connected by flow lines of $\psi_*(\phi)$ near a critical point are in $\mathcal{N}$. ◇

Similarly, we have

Lemma 6.8

$$\lim_{\varepsilon \to 0} \Psi(P_{\mathcal{I}}) \cap \iota(P_\phi) = \sum_{c \in \mathcal{C}} \mathcal{J}_{j(c)i(c)}(-\sigma(c))\overline{\{(\gamma(c)(t_1), \gamma(c)(t_2)); t_1 > t_2\}} + O(\mathcal{N}).$$

PROOF: Away from the unit bundles of the critical points, it is clear. According to Lemma 6.2, the direction of $\overline{\phi}$ on $\psi(\mathcal{A}_i)$ near $\psi(a_i)$ (or on $\psi(\mathcal{B}_j)$ near $\psi(b_j)$) is in the hemisphere centered at $\sigma_a(-Y)$, so that the pairs of points of $(\psi(\mathcal{B}_j) \times \psi(\mathcal{A}_i)) \cap \iota(P_\phi)$ near the critical points are again in $\mathcal{N}$. ◇

Proposition 6.4 is a direct corollary of Lemmas 6.3, 6.6, 6.7, 6.8. ◇

6.6 Proof of Proposition 6.5

We prove that $\left(\mathcal{P}_X \cap \mathcal{P}_{-X} \cap ([0, 5/2] \times \partial C_2(M))\right)$ is in $\mathcal{N}$.

According to Theorem 4.2,

$$\partial \mathcal{P}(f, \mathfrak{g}) = \partial_{od} + \sum_{c \in \mathcal{C}} \mathcal{J}_{j(c)i(c)} \sigma(c)(S^2 \times \gamma(c)) + \overline{s_\phi(\check{M})}.$$

Therefore, according to Lemmas 6.3 and 6.2,

$$\Psi(\partial \mathcal{P}(f, \mathfrak{g})) \cap \partial \iota(\mathcal{P}(f, \mathfrak{g})) = O(\mathcal{N}).$$

Let us now show that

$$\Psi(\partial \mathcal{P}(f, \mathfrak{g})) \cap \iota(P_h) = O(\mathcal{N}).$$

According to the construction of P_h in Subsections 5.1 and 5.2, $\iota(P_h)$ intersects $\Psi(S^2 \times \gamma(c)) = S^2 \times \psi(\gamma(c))$ on $s_{[\overline{\phi}, -X]}(\psi(\gamma(c))$ where $[\overline{\phi}, -X]$ is the shortest geodesic arc between the tangent to $\overline{\phi}$ and $-X$, which is in the hemisphere centered at $\sigma_a(-Y)$,

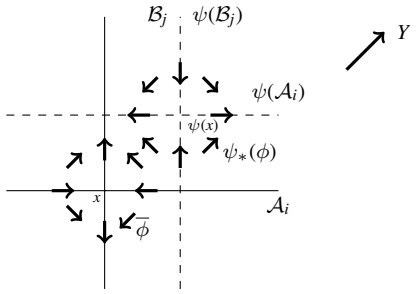

Figure 18: Tangencies of the flow lines of $\overline{\phi}$ and $\psi_*(\phi)$ near some $\gamma(c)$

according to Lemma 6.2. Now, look at the intersection of $\iota(P_h)$ and $s_{\psi_*(\phi)}(\check{M})$, where the direction of $\psi_*(\phi)$ must belong to $[\overline{\phi}, -X]$. This can only happen in a tubular neighborhood of γ_i at a place where the flow lines of $\psi_*(\phi)$ and $\overline{\phi}$ have the same horizontal direction. This only happens between γ_i and $\psi(\gamma_i)$, more precisely in the preimage of the rectangle shown in Figure 18 under the orthogonal projection directed by X_1. There the horizontal direction is close to the direction of $\sigma_a(-Y)$.

Similarly,

$$\Psi(P_h) \cap \left(S^2 \times L + \overline{(-X)(\check{M})}\right) = O(\mathcal{N}).$$

Indeed, since the horizontal component of the direction of $\psi_*(\phi)$ along $\gamma(c)$ is in the direction of $\sigma_a(-Y)$, $\Psi(P_h) \cap (S^2 \times L) = O(\mathcal{N})$. Now, $(-X)$ can belong to $[\psi_*(\phi), \psi_*(X)]$ only if the direction of the horizontal component of $(-X)$, which is the direction of horizontal component of $s_{\overline{\phi}}$, is the same as the direction of the horizontal component of $s_{\psi_*(\phi)}$. This can only happen in the same rectangles as before where $(-X)$ is in the hemisphere centered at $\sigma_a(-Y)$. Finally,

$$\Psi(-S^2 \times L + \overline{X(\check{M})}) \cap \left(S^2 \times L + \overline{(-X)(\check{M})}\right) = O(\mathcal{N})$$

since it only consists of unit tangent vectors to $\check{M}$ over $L \cup \psi(L)$ in the direction of $\pm X$. ◇

7 Concluding the proof of Theorem 3.8

Recall that w, $\mathfrak{m}$, $X = X(w, \mathfrak{m})$, $L = L(\mathfrak{m})$ and Σ such that $\partial\Sigma = L$ are fixed. Note that X depends neither on the orientations of the α_i and the β_j, nor on their order. Furthermore $e(w, \mathfrak{m})$ is independent of the order of the β_j. Thus, the permutation ρ of $\{1, 2, \dots, g\}$ associated with $\mathfrak{m}$ is assumed to be the identity, without loss.

7.1 Reducing the proof of Theorem 3.8 to an Euler class computation

Define four nowhere zero fields Y^{++}, Y^{+-}, ($Y^{-+} = -Y^{+-}$) and ($Y^{--} = -Y^{++}$) of $X^{\perp}$, up to homotopy among nowhere zero fields, over a neighborhood of the $\gamma(c)$, so that

- Y^{++} and Y^{+-} are *positive normals* for $\mathcal{A}_i$ on $H_{a,\leq 3} = C_M \cap f^{-1}(]-\infty, 3])$ –meaning that Y^{++} (or Y^{+-}) followed by an oriented basis of the tangent space to $\mathcal{A}_i$ gives rise to an oriented basis of the tangent space to M–, and
- Y^{++} and Y^{-+} are positive normals for $\mathcal{B}_j$ on $H_{b,\geq 3} = C_M \cap f^{-1}([3, +\infty[)$,

Figure 19: The fields $Y^{\varepsilon,\eta}$ on $f^{-1}(\{3\})$

More explicitly, such fields $Y^{\varepsilon,\eta}$ can be pictured on $f^{-1}(\{3\})$ as in Figure 19 and the field Y^{++} becomes closer to the "actual positive orthogonal normal" of $\mathcal{A}_i$ as we approach a_i, and closer to the "actual positive orthogonal normal" of $\mathcal{B}_j$, as we approach b_j, where Figure 19 cannot be drawn anymore. (In order to determine these fields up to homotopy among nowhere zero fields, it is enough to determine an open half-space where they lie, continuously.)

Then with the notation of Subsections 3.2 and 3.5,

$$lk(L(\mathfrak{m}), L(\mathfrak{m})_{\|}) = \frac{1}{4} \sum_{(\varepsilon,\eta)\in\{+,-\}^2} lk(L, L_{\|Y^{\varepsilon,\eta}})$$

and, with the notation of Proposition 6.1,

$$[G_{\uparrow\downarrow}] = \frac{1}{4} \sum_{(\varepsilon,\eta)\in\{+,-\}^2} \left[G^i_{\uparrow\downarrow}(Y^{\varepsilon,\eta}) + G^b_{\uparrow\downarrow}(X, Y^{\varepsilon,\eta})\right]$$

where $\sigma_a(-Y^{\varepsilon,\eta}) = Y^{\varepsilon,(-\eta)}$, so that the collection of the $\sigma_a(-Y^{\varepsilon,\eta})$ is the same as the collection of the $Y^{\varepsilon,\eta}$ and, thanks to Lemma 4.1,

$$[G(\mathcal{D})] = \frac{1}{4} \sum_{(\varepsilon,\eta)\in\{+,-\}^2} [G^i_{\uparrow\downarrow}(Y^{\varepsilon,\eta})]$$

with the notation of Proposition 3.2.

Therefore, thanks to Proposition 6.1, the proof of Theorem 3.8 is reduced to the proof of the following equality in $H_2(U\check{M};\mathbb{Q})$.

$$\left[X(\Sigma)-(-X)(\Sigma)-\frac{1}{4}\sum_{(\varepsilon,\eta)\in\{+,-\}^2} s_{[-X,X]_{Y^{\varepsilon},\eta}}(\partial\Sigma)\right]=e(w,\mathfrak{m})[S].$$

Consider the rank 2 sub-vector bundle $X^\perp$ of $T\check{M}$ of the planes orthogonal to X. Let $X^\perp(\Sigma)$ be the total space of the restriction of $X^\perp$ to our surface Σ. Let Y be a nowhere zero section of $X^\perp$ on $\partial\Sigma$. The *relative Euler class* $e(X^\perp(\Sigma),Y)$ *of* Y *in* $X^\perp(\Sigma)$ is the obstruction to extending Y as a nonzero section of $X^\perp(\Sigma)$ over Σ. If $\tilde{Y}$ is an extension of Y as a section of $X^\perp(\Sigma)$ transverse to the zero section $s_0(X^\perp(\Sigma))$, then

$$e(X^\perp(\Sigma),Y)=\langle\tilde{Y}(\Sigma),s_0(X^\perp(\Sigma))\rangle_{X^\perp(\Sigma)}.$$

Lemma 7.1 *Under the assumptions above,*

$$\left[X(\Sigma)-(-X)(\Sigma)-s_{[-X,X]_Y}(\partial\Sigma)\right]=e(X^\perp(\Sigma),Y)[S]$$

in $H_2(C_2(M))$.

PROOF: If Y extends as a nonzero section of $X^\perp(\Sigma)$ still denoted by Y, then the cycle of the left-hand side bounds $s_{[-X,X]_Y}(\Sigma)$. This allows us to reduce the proof to the case when Σ is a neighborhood of a zero of the extension $\tilde{Y}$ above, that is when Σ is a disk Δ equipped with a trivial D^2-bundle, and when $Y\colon\partial\Delta\to\partial D^2$ has degree $d=\pm1$. Then $d=e(X^\perp(\Delta),Y)$, and $\left[X(\Delta)-(-X)(\Delta)-s_{[-X,X]_Y}(\partial\Delta)\right]=d[S]$. ◇

Thus,

$$\left[X(\Sigma)-(-X)(\Sigma)-\frac{1}{4}\sum_{(\varepsilon,\eta)\in\{+,-\}^2} s_{[-X,X]_{Y^{\varepsilon},\eta}}(\partial\Sigma)\right]$$
$$=\frac{1}{4}\sum_{(\varepsilon,\eta)\in\{+,-\}^2} e(X^\perp(\Sigma),Y^{\varepsilon,\eta})[S].$$

The proof of Theorem 3.8 is now reduced to the proof of the following proposition, which occupies the end of this section.

Proposition 7.2

$$e(w,\mathfrak{m})=\frac{1}{4}\sum_{(\varepsilon,\eta)\in\{+,-\}^2} e(X(w,\mathfrak{m})^\perp(\Sigma),Y^{\varepsilon,\eta}).$$

Remark 7.3 Note that this proposition provides a combinatorial formula for the average of the Euler classes in the right-hand side. In this formula, the $d_e(\beta_j)$ and $d_e(|c_{j(c)}, c|_\beta)$ depend on our rectangular diagram of $(\mathcal{D}, \mathfrak{m}, w)$ in Figure 3. Thus, the proposition implies that the sum $e(w, \mathfrak{m})$ is independent of our special picture of the Heegaard diagram.

7.2 A surface $\Sigma(L(\mathfrak{m}))$

Let $H_{b,\geq 2} = C_M \cap f^{-1}([2, +\infty[)$. For any crossing c of $\mathcal{C}$, define the triangle $T_\beta(c)$ in the disk $(D_{\geq 2}(\beta_{j(c)}) = \mathcal{B}_{j(c)} \cap H_{b,\geq 2})$ such that

$$\partial T_\beta(c) = [c_{j(c)}, c]_\beta + (\gamma(c) \cap H_{b,\geq 2}) - (\gamma_{j(c)} \cap H_{b,\geq 2}).$$

Similarly, define the triangle $T_\alpha(c)$ in the disk $(D_{\leq 2}(\alpha_{i(c)}) = \mathcal{A}_{i(c)} \cap H_a)$ such that

$$\partial T_\alpha(c) = -[c_{i(c)}, c]_\alpha + (\gamma(c) \cap H_a) - (\gamma_{i(c)} \cap H_a).$$

Proposition 7.4 *Recall $H_{a,2} = C_M \cap f^{-1}(2)$. There exists a 2-chain $F(\mathfrak{m})$ in $H_{a,2}$ such that the boundary of*

$$\Sigma(L(\mathfrak{m})) = F(\mathfrak{m}) - \sum_{c\in\mathcal{C}} \mathcal{J}_{j(c)i(c)}\sigma(c)(T_\beta(c) + T_\alpha(c))$$

$$+ \sum_{(j,i)\in\{1,\dots,g\}^2} \sum_{c\in\mathcal{C}} \mathcal{J}_{j(c)i(c)}\sigma(c)\mathcal{J}_{ji}\left(\langle\alpha_i, |c_{j(c)}, c|_\beta\rangle D_{\geq 2}(\beta_j) - \langle|c_{i(c)}, c|_\alpha, \beta_j\rangle D_{\leq 2}(\alpha_i)\right)$$

is $L(\mathfrak{m})$.

PROOF: The boundary of the defined pieces reads $(L(\mathfrak{m}) + u)$ where the cycle u is

$$\begin{aligned} u = \quad & \textstyle\sum_{c\in\mathcal{C}} \mathcal{J}_{j(c)i(c)}\sigma(c)\left([c_{i(c)}, c]_\alpha - [c_{j(c)}, c]_\beta\right) \\ & + \textstyle\sum_{(j,i)\in\{1,\dots,g\}^2} \sum_{c\in\mathcal{C}} \mathcal{J}_{j(c)i(c)}\sigma(c)\mathcal{J}_{ji}\left(\langle\alpha_i, |c_{j(c)}, c|_\beta\rangle\beta_j - \langle|c_{i(c)}, c|_\alpha, \beta_j\rangle\alpha_i\right). \end{aligned}$$

Compute $\langle\alpha_k, u\rangle$, by pushing u in the direction of the positive normal to α_k and in the direction of the negative normal, and by averaging. Since α_k intersects neither the pushed $[c_{i(c)}, c]_\alpha$ nor the pushed α_i, and since its intersection with the above average of the pushed $[c_{j(c)}, c]_\beta$ is $\langle\alpha_k, |c_{j(c)}, c|_\beta\rangle$,

$$\langle\alpha_k, u\rangle = -\sum_{c\in\mathcal{C}} \mathcal{J}_{j(c)i(c)}\sigma(c)\langle\alpha_k, |c_{j(c)}, c|_\beta\rangle + \sum_{c\in\mathcal{C}} \mathcal{J}_{j(c)i(c)}\sigma(c)\langle\alpha_k, |c_{j(c)}, c|_\beta\rangle = 0.$$

Similarly, $\langle u, \beta_\ell\rangle = 0$ for any ℓ so that $(-u)$ bounds a 2-chain $F(\mathfrak{m})$ in $H_{a,2}$. $\diamond$

7.3 Proof of the combinatorial formula for the Euler classes

In this section, we prove Proposition 7.2.

Represent H_a like in Figure 7, and assume that the curves β_j intersect the handles as arcs parallel to Figure 20, one below through the favourite crossing and the other ones above.

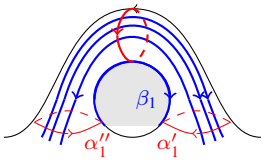

Figure 20: How the β_j look like near the handles' cores

For each α_i, remove the annular neighborhood of α_i bounded by $\alpha_i'' \cup (-\alpha_i')$ in Figure 20 from $H_{a,2}$ in order to get the rectangular diagram of $(\mathcal{D}, \mathfrak{m}, w)$ of Figure 3, Subsection 3.5.

Let $H_{a,2}^{\mathfrak{m}}$ denote the complement of disk neighborhoods of the favourite crossings in the surface $H_{a,2}$. See $H_{a,2}^{\mathfrak{m}}$ as the surface obtained from the rectangle of Figure 3 by adding a band of the handle's upper part for each α_i, so that the band of α_i contains all the non-favourite crossings of α_i. See Figure 21 for an immersion of this surface in the plane.

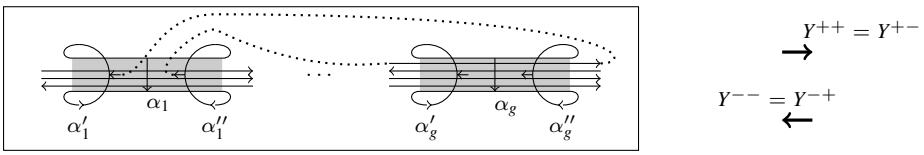

Figure 21: The punctured surface $H_{a,2}^{\mathfrak{m}}$

Extend every $Y = Y^{\varepsilon,\eta}$ on H_a so that the fields $Y^{\varepsilon,\eta}$ are horizontal and their projections are the depicted constant fields in Figure 21.

Note that $[0, 2g] \times [0, 4] \times [-\infty, 0]$ is the product of Figure 22 by $[-\infty, 0]$ where all the flow lines are directed by $[-\infty, 0]$.

Similarly, assume that the α-curves are orthogonal to the picture on the lower parts of the handles in the standard picture of H_b in Figure 7, and draw a planar picture similar to Figure 21 of $H_{a,4}^{\mathfrak{m}}$ (which is $f^{-1}(4) \cap C_M$ minus disk neighborhoods of the favourite

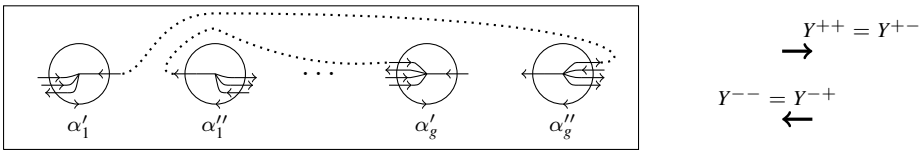

Figure 22: A typical slice of $[0,2g]\times[0,4]\times[-\infty,0]$

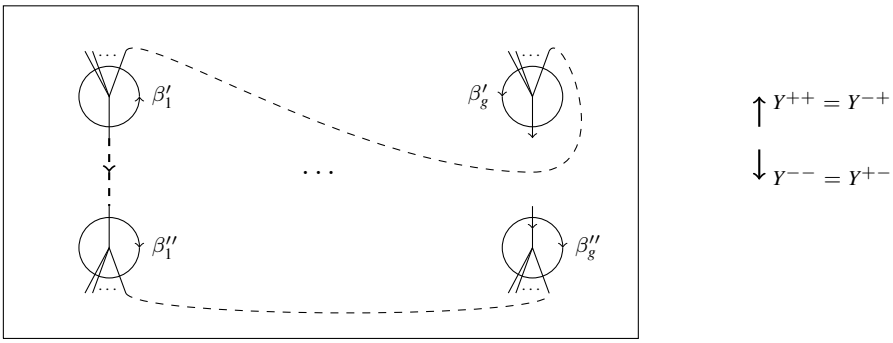

Figure 23: A typical slice of $[0,2g]\times[0,4]\times[6,\infty]$

crossings), by starting with Figure 23 and by adding a vertical band cut by a horizontal arc of β_j oriented from right to left, for each β_j.

Again, $[0,2g]\times[0,4]\times[6,\infty]$ is the product of Figure 23 by $[6,\infty]$ where all the flow lines are directed by $[6,\infty]$. Extend every $Y = Y^{\varepsilon,\eta}$ on H_b so that Y looks constant and horizontal in our standard figure of H_b in Figure 7 and so that its projection on Figure 23 is the drawn constant field.

Also assume that every $Y = Y^{\varepsilon,\eta}$ varies in a quarter of horizontal plane in our tubular neighborhoods of the γ_i in Figure 14. Similarly, extend every $Y = Y^{\varepsilon,\eta}$ in the product by $[2,4]$ of the bands of Figure 21 so that $Y^{\varepsilon,\eta}$ is horizontal and is never a $(-\varepsilon)$-normal to the $\mathcal{A}_i$ there.

Let $H^{\mathcal{C}}_{a,2}$ denote the punctured rectangle of Figure 3, which is a subsurface of $H_{a,2}$. Now, Y is defined everywhere except in $H^{\mathcal{C}}_{a,2}\times]2,4[$ so that, for the surface $\Sigma = \Sigma(L(\mathfrak{m}))$ of Proposition 7.4,

$$e(X^\perp(\Sigma),Y) = e(X^\perp(\Sigma\cap(H^{\mathcal{C}}_{a,2}\times[2,4])),Y)$$

$$\begin{aligned} = \ & -\textstyle\sum_{c\in\mathcal{C}} \mathcal{J}_{j(c)i(c)}\sigma(c)e(X^\perp([c_{j(c)},c]_\beta\times[2,4])),Y) \\ & +\textstyle\sum_{(j,i)\in\{1,\dots,g\}^2}\sum_{c\in\mathcal{C}} \mathcal{J}_{j(c)i(c)}\sigma(c)\mathcal{J}_{ji}\langle\alpha_i,|c_{j(c)},c|_\beta\rangle e(X^\perp(\beta_j\times[2,4]),Y). \end{aligned}$$

Thus, Proposition 7.2 will be proved as soon as we have proved the following lemma.

Lemma 7.5 *With the notation of Subsection 3.5,*

$$d_e(\beta_j) = -\frac{1}{4} \sum_{(\varepsilon,\eta)\in\{+,-\}^2} e(X^\perp(\beta_j \times [2,4]), Y^{\varepsilon,\eta})$$

and

$$d_e(|c_{j(c)}, c|_\beta) = -\frac{1}{4} \sum_{(\varepsilon,\eta)\in\{+,-\}^2} e(X^\perp(|c_{j(c)}, c|_\beta \times [2,4]), Y^{\varepsilon,\eta}).$$

PROOF: Consider an arc $[c,d]_\beta$ between two consecutive crossings of β. Let $[c',d'] = [c,d]_\beta \cap H^C_{a,2}$. On $[c',d'] \times [2,4]$, the field X is directed by $[2,4]$, the field $Y^{\varepsilon,\eta}$ is defined on $\partial\left([c',d'] \times [2,4]\right)$, and it is in the hemisphere of the η-normal to $[c',d'] \times [2,4]$ along $\partial\left([c',d'] \times [2,4]\right) \setminus [c',d'] \times \{2\}$ (the η-normal is the positive normal when $\eta = +$ and the negative normal otherwise). Then $e(X^\perp([c',d'] \times [2,4]), Y^{\varepsilon,\eta})$ is the degree of $Y^{\varepsilon,\eta}$ at the $(-\eta)$-normal to $[c',d'] = [c',d'] \times \{2\}$, in the fiber of the unit tangent bundle $UH_{a,2}$ of $H_{a,2}$ trivialised by the normal to $[c',d']$. Thus, $e(X^\perp([c',d'] \times [2,4]), Y^{\varepsilon,\eta})$ is the opposite of the degree of the $(-\eta)$-normal to $[c',d']$ in the fiber of $UH_{a,2}$ at $Y^{\varepsilon,\eta}$ trivialised by $Y^{\varepsilon,\eta}$ (that is by Figure 3) along $[c',d']$. This $(-\eta)$-normal starts and ends as vertical in this figure, and $Y^{\varepsilon,\eta}$ is horizontal with a direction that depends on the sign of ε. The $(-\eta)$-normal to $[c',d']$ makes $(d_e(|c,d|_\beta) \in \frac{1}{2}\mathbb{Z})$ positive loops with respect to the parallelization induced by Figure 3. Therefore the sum of the degrees of the $(-\eta)$ normal at the direction of $Y^{\varepsilon,\eta}$ and at the direction of $Y^{(-\varepsilon),\eta}$ is $2d_e(|c,d|_\beta)$.

This shows that

$$\begin{aligned} d_e(|c,d|_\beta) &= -\tfrac{1}{2}\left(e(X^\perp([c',d'] \times [2,4]), Y^{\varepsilon,\eta}) + e(X^\perp([c',d'] \times [2,4]), Y^{(-\varepsilon),\eta})\right) \\ &= -\tfrac{1}{4}\textstyle\sum_{(\varepsilon,\eta)\in\{+,-\}^2} e(X^\perp([c',d'] \times [2,4]), Y^{\varepsilon,\eta}). \end{aligned}$$

The first equality of the statement follows since each side is the sum, over all the arcs of β_j between consecutive crossings, of the corresponding side of the equality above. The second equality follows similarly. This concludes the proof of Lemma 7.5, and therefore the proofs of Proposition 7.2 and Theorem 3.8. ◇

Index of notations

References

[1] **Selman Akbulut, John D McCarthy**, *Casson's invariant for oriented homology 3-spheres*, volume 36 of *Mathematical Notes*, Princeton University Press, Princeton, NJ (1990), an exposition

[2] **Robert E Gompf**, *Handlebody construction of Stein surfaces*, Ann. of Math. (2) 148 (1998) 619–693, URL http://dx.doi.org/10.2307/121005

[3] **Lucien Guillou, Alexis Marin**, *Notes sur l'invariant de Casson des sphères d'homologie de dimension trois*, Enseign. Math. (2) 38 (1992) 233–290, with an appendix by Christine Lescop

[4] **Morris W Hirsch**, *Differential topology*, volume 33 of *Graduate Texts in Mathematics*, Springer-Verlag, New York (1994), corrected reprint of the 1976 original

[5] **Friedrich E P Hirzebruch**, *Hilbert modular surfaces*, Enseignement Math. (2) 19 (1973) 183–281

[6] **Rob Kirby, Paul Melvin**, *Canonical framings for 3-manifolds*, from: "Proceedings of 6th Gökova Geometry-Topology Conference", Turkish J. Math. 23 (1999) 89–115

[7] **Maxim Kontsevich**, *Feynman diagrams and low-dimensional topology*, from: "First European Congress of Mathematics, Vol. II (Paris, 1992)", Progr. Math. 120, Birkhäuser, Basel (1994) 97–121

[8] **Greg Kuperberg, Dylan Thurston**, *Perturbative 3–manifold invariants by cut-and-paste topology* (1999), URL http://arxiv.org/abs/math/9912167, math.GT/9912167

[9] **Thang T Q Le, Jun Murakami, Tomotada Ohtsuki**, *On a universal perturbative invariant of 3-manifolds*, Topology 37 (1998) 539–574, URL http://dx.doi.org/10.1016/S0040-9383(97)00035-9

[10] **Christine Lescop**, *On the Kontsevich-Kuperberg-Thurston construction of a configuration-space invariant for rational homology 3-spheres* (2004), URL http://arxiv.org/abs/math/0411088, math.GT/0411088

[11] **Christine Lescop**, *Splitting formulae for the Kontsevich-Kuperberg-Thurston invariant of rational homology 3-spheres* (2004), URL http://arxiv.org/abs/math/0411431, math.GT/0411431

[12] **Christine Lescop**, *Introduction to finite type invariants of knots and 3–manifolds* (2013), URL http://arxiv.org/abs/1312.2566, arXiv:1312.2566v1

[13] **Christine Lescop**, *On homotopy invariants of combings of 3–manifolds* (2013), URL http://arxiv.org/abs/1209.2785, arXiv:1209.2785v2, to appear in Canadian Journal of Mathematics

[14] **Christine Lescop**, *A combinatorial definition of the Θ-invariant from Heegaard diagrams* (2014), URL http://arxiv.org/abs/1402.2261, arXiv:1402.2261

[15] **Alexis Marin**, *Un nouvel invariant pour les sphères d'homologie de dimension trois (d'après Casson)*, Astérisque (1988) Exp. No. 693, 4, 151–164 (1989), séminaire Bourbaki, Vol. 1987/88

[16] **Kevin Walker**, *An extension of Casson's invariant*, volume 126 of *Annals of Mathematics Studies*, Princeton University Press, Princeton, NJ (1992)

[17] **Tadayuki Watanabe**, *Higher order generalization of Fukaya's Morse homotopy invariant of 3-manifolds I. Invariants of homology 3-spheres* (2012), URL http://arxiv.org/abs/1202.5754, arXiv:1202.5754v2

[18] **Edward Witten**, *Quantum field theory and the Jones polynomial*, Comm. Math. Phys. 121 (1989) 351–399, URL http://projecteuclid.org/getRecord?id=euclid.cmp/1104178138

Institut Fourier, UJF Grenoble, CNRS, 100 rue des maths, BP 74, 38402 Saint-Martin d'Hères cedex

Christine.Lescop@ujf-grenoble.fr

http://www-fourier.ujf-grenoble.fr/~lescop/